Cancer Letters 588 (2024) 216776

Contents lists available at ScienceDirect

Cancer Letters

journal homepage: www.elsevier.com/locate/canlet

Original Articles

CRISPR/Cas9 screenings unearth protein arginine methyltransferase 7 as a novel essential gene in prostate cancer metastasis

Maria Rodrigo-Faus [a,b], Africa Vincelle-Nieto [c], Natalia Vidal [d], Javier Puente [d], Melchor Saiz-Pardo [d], Alejandra Lopez-Garcia [e], Marina Mendiburu-Eliçabe [f], Nerea Palao [a,b], Cristina Baquero [a,b], Paula Linzoain-Agos [a,b], Angel M. Cuesta [a,b], Hui-Qi Qu [g], Hakon Hakonarson [g,h], Monica Musteanu [a,e,i], Armando Reyes-Palomares [c], Almudena Porras [a,b], Paloma Bragado [a,b], Alvaro Gutierrez-Uzquiza [a,b,*]

[a] Department of Biochemistry and Molecular Biology, Pharmacy Faculty, Complutense University of Madrid, Madrid, Spain
[b] Health Research Institute of the Clínico San Carlos Hospital (IdISSC), Madrid, Spain
[c] Department of Biochemistry and Molecular Biology, Veterinary Faculty, Complutense Univeristy of Madrid, Madrid, Spain
[d] Department of Medical Oncology, Health Research Institute of the Clínico San Carlos Hospital (IdISSC), CIBERONC, Madrid, Spain
[e] Experimental Oncology, Molecular Oncology Program, Spanish National Cancer Research Center (CNIO), Madrid, Spain
[f] Molecular and Cellular Biology of Cancer Institute (IBMCC-CIC), Salamanca, Spain
[g] Center for Applied Genomics (CAG), Children's Hospital of Philadelphia, Philadelphia, PA, 19104, USA
[h] Department of Pediatrics, The Perelman School of Medicine, University of Pennsylvania, Philadelphia, PA, 19104, USA
[i] Cancer and Obesity Group, Health Research Institute of the Clínico San Carlos Hospital (IdISSC), Madrid, Spain

ARTICLE INFO

Keywords:
Prostate cancer
Metastasis
Invasion
PRMT7
Adhesion

ABSTRACT

Due to the limited effectiveness of current treatments, the survival rate of patients with metastatic castration-resistant prostate cancer (mCRPC) is significantly reduced. Consequently, it is imperative to identify novel therapeutic targets for managing these patients. Since the invasive ability of cells is crucial for establishing and maintaining metastasis, the aim of this study was to identify the essential regulators of invasive abilities of mCRPC cells by conducting two independent high-throughput CRISPR/Cas9 screenings. Furthermore, some of the top hits were validated using siRNA technology, with protein arginine methyltransferase 7 (PRMT7) emerging as the most promising candidate. We demonstrated that its inhibition or depletion via genetic or pharmacological approaches significantly reduces invasive, migratory and proliferative abilities of mCRPC cells *in vitro*. Moreover, we confirmed that *PRMT7* ablation reduces cell dissemination in chicken chorioallantoic membrane and mouse xenograft assays. Molecularly, PRMT7 reprograms the expression of several adhesion molecules by methylating various transcription factors, such as FoxK1, resulting in the loss of adhesion from the primary tumor and increased motility of mCRPC cells. Furthermore, *PRMT7* higher expression correlates with tumor aggressivity and poor overall survival in prostate cancer patients. Thus, this study demonstrates that *PRMT7* is a potential therapeutic target and potential biomarker for mPCa.

1. Introduction

PCa remains the second most frequent cancer and the fifth leading cause of cancer deaths among men [1]. While most PCa patients are initially diagnosed with localized androgen-sensitive tumors, some will eventually progress to metastatic castration resistant prostate cancer (mCRPC), which is unresponsive to standard androgen-deprivation hormonal therapy and have a limited response to conventional chemotherapy [2,3]. As a result, the survival rate of mCRPC patients is less than 3 years [4]. Hence, there is an urge to find new actionable targets and biomarkers to establish effective therapies to manage mCRPC patients increasing their survival.

Despite the alarming number of deaths from metastatic cancer each year, metastasis appearance is still poorly understood. Some biological

* Corresponding author. Department of Biochemistry and Molecular Biology, Faculty of Pharmacy, Complutense University of Madrid, Plaza Ramón y Cajal s/n, 28040, Madrid, Spain.
E-mail address: alguuz@ucm.es (A. Gutierrez-Uzquiza).

https://doi.org/10.1016/j.canlet.2024.216776
Received 7 November 2023; Received in revised form 19 February 2024; Accepted 29 February 2024
Available online 2 March 2024

changes have been described to be crucial in promoting localized primary tumor progression to a secondary foci dissemination stage. They involve primary tumor cell adhesion loss, degradation of the basement membrane, intravasation to the circulatory system, survival in the bloodstream, extravasation into a distant organ and generation of a new tumor bulk [5].

Metastatic tumor cells display high levels of genomic instability and harbor several epigenetic alterations that may empower them with disseminative abilities to generate a new tumor burden. While the exact mPCa gene signature remains unknown, mPCa cancer cells frequently bear alterations in androgen-receptor (AR) signaling [6], deletions in *TP53, RB1* and *PTEN* genes, overactivated Akt signaling, *ETS* gene rearrangements and deleterious mutations in some DNA-repair genes such as *BRCA2* [7,8]. Moreover, some studies also highlight the importance of epigenetic factors such as *EZH2*, which ectopic overexpression correlates with metastasis and poor prognosis in PCa patients [9]. Nonetheless, much remains to be investigated to fully understand the mechanisms that enhance the migratory and invasive abilities of PCa tumor cells.

Some single-gene studies have unearthed metastatic prostate cancer regulators such as *WNT5A* [10], *MAP4K4* [11] or *PPP1CA* [12]. However, given the complexity of the biological mechanisms implicated in metastasis, unbiased high-throughput CRISPR/Cas9 screening assays seem a powerful tool for uncovering new targetable regulators of cell invasion in mCRPC. This approach is based on CRISPR/Cas9 genome editing that makes it possible to selectively modify the genome [13]. Zhang lab [14] have developed Cas9/guide RNAs (gRNAs) libraries using lentiviruses that can facilitate both positive and negative loss-of-function (LOF) screenings in mammalian cells. *In vitro* and *in vivo* CRISPR screenings have been successfully performed during the last years in different cancer models, including leukemia and lung cancer [15,16] proving its usefulness to find novel relevant oncogenes. Therefore, the aim of this study is to conduct high-throughput *in vitro* screening assays, using the human GeCKO CRISPR/Cas9 library [14], to identify essential genes and biological processes for metastasis in mCRPC cellular models with the purpose of establishing new actionable targets and/or biomarkers of mCRPC.

Briefly, our CRISPR/Cas9 screenings identified the protein arginine methyltransferase 7 (*PRMT7*) as an essential gene for the invasive abilities of PC3 and DU145 cells. Its depletion via genetic and pharmacological approaches significantly decreased invasive, migratory and proliferative capacities of mCRPC cellular models. Moreover, PC3 cells genetically engineered to abolish *PRMT7* expression showed a reduced dissemination ability *in vivo*. Further investigation demonstrated that PRMT7 induces a switch in the expression of cellular adhesion molecules, mediated through FoxK1, LXR-β and/or NCOA2/3 transcription factors methylation. Importantly, *PRMT7* higher expression correlates with tumor aggressivity and poor overall survival of prostate cancer patients. Therefore, our data supports a metastasis promoting role for *PRMT7* in mCRPC and a potential application as a new therapeutic target.

2. Materials and methods

2.1. Cell culture and reagents

PC3 (CRL-1435) and DU145 (HTB-81) cell lines were obtained from ATCC and cultured in RPMI/HAM'S F12 10% FBS and RPMI 10% FBS medium, respectively. HEK293T (CRL-3216) cells obtained from ATCC, were cultured in 10% FBS DMEM medium and were used for lentiviral production.

2.2. CRISPR/Cas9 library preparation

LentiCRISPR v2 GeCKO Human library (Addgene plasmid #52961) was amplified following Sanjana NE et al., protocol [14]. Lenti-Cas9 viral production was performed in HEK293T cells. A mixture of the 3 transfection plasmids, packaging and enveloping plasmids psPAX2 (addgene#12260) and pMD2.VSVg (addgene#8454), together with lentiCas9-Blast plasmid (addgene#52962) was prepared and mixed with lipofectamine 2000 (Invitrogen) in a 1:3 ratio and transferred to the HEK293T cells. After 72h, the medium was collected, centrifuged at 2000 rpm for 5 min, and filtered with a 0.45 μm pore syringe filter. PC3 and DU145 cells were transduced with lenti-Cas9 virus to induce the expression of Cas9 in presence of 8 μg/mL of polybrene. 48h later, blasticidine selection (10 μg/ml) was performed for 5 days. Individual clones were expanded and the Cas9 presence was verified by western blot using Cas9 anti-mouse IgG (14697S, CST) and proliferation and migration tests were performed to ensure no clonal effect (data not shown). Subsequently, a mixture of the 3 transfection plasmids, packaging and enveloping plasmids psPAX2 (addgene#12260) and pMD2.VSVg (addgene#8454), together with the gRNA from library A (targeting 20,000 genes, including 1,864 gRNA microRNA and 1,000 non-targeting controls) [14] was prepared and mixed with lipofectamine 2000 in a 1:3 ratio and transferred to the HEK293T cells. After 72h, the medium was collected, centrifuged at 2000 rpm for 5 min and filtered with a 0.45 μm pore syringe filter. PC3-Cas9 and DU145-Cas9 cells were transduced with lentivirus containing the pre-designed gRNAs in presence of 8 μg/mL of polybrene. 48h later, puromycin selection (10 μg/mL) was performed for 5 days. Next, an invasion assay in Matrigel-coated Boyden chambers was conducted, separately for both cell lines, to investigate which genes were more essential to the invasive process, key in mPCa onset.

2.3. MAGeCK screening analysis

DNA from the population of cells in the upper chamber of the Matrigel-coated Boyden Chamber membrane and the population of cells in the bottom of it, was isolated separately. Specific primers designed to amplify all the gRNAs included in the lentiCRISPR v2 GeCKO Human library (Supplementary Table 1) were used to amplify these sequences that were included in the DNA of the cells through lentiviral infection. Subsequently, Next Generation Sequencing (NGS) was performed at Genomic and genetic facility at UCM and analysis of raw data was conducted at Bioinformatics for Genomics and Proteomics Unit at CNB–CSIC facility (Madrid, Spain) using MAGeCK algorithm [17]. To proceed with further analysis, we discarded the genes where only 1 gRNA was detected by NGS, to improve the reliability of the screening results.

2.4. Gene silencing by small interfering RNA

Predesigned siRNAs were obtained from Dharmacon (Supplementary Table 1). 2.5×10^5 cells were initially transfected with 50 nM of siRNA using lipofectamine RNAiMAX following manufacturer's protocol (Invitrogen). After 48h of incubation, cells were used for invasion or immunoblot assays.

2.5. PRMT7 CRISPR/Cas9 knock-out production

Lenti-g*PRMT7* and lenti-gControl was performed as previously described [11], using the specific gRNA for *PRMT7* (forward 5′-*CACCG*AAGGCCTTGGTTCTCGACAT-3′ and reverse 5′-*AAA*CATGTCGAGAACCAAGGCCTTC-3′) or for the control (gCTL) (forward 5′- *CACCG* CGGCTGAGGCACCTGGTTTA-3′ and reverse 5′-*AAA*CTAAACCAGGTGCCTCAGCCG-3′). PC3-Cas9 and DU145-Cas9 previously engineered in the laboratory, were infected with *gPRMT7* or gCTL in presence of polybrene (8 μg/mL). After 48h, puromycin selection (10 μg/mL) was added for 5 days. A serial dilution was performed in 96 multi-well plates to obtain single cell clones. *PRMT7* knock-out was confirmed by western-blot using anti-PRMT7 antibody and by sanger sequencing (data not shown).

2.6. Protein extraction and immunoblotting

Cells were lysed and western blot protocol was carried out as previously described [18]. Primary antibodies used were β-Actin (sc-47778, Santa Cruz Biotechnology), PRMT7 (#14762S, CST), Mono-Methyl Arginine (Me-R4-100, CST) (#8015S, CST), PRMT5 (sc-376937, Santa Cruz Biotechnology), ITGα1 (sc-271034, Santa Cruz Biotechnology) or ITGβ4 (sc-9090, Santa Cruz Biotechnology). Secondary antibodies used were anti-mouse IgG (NA931, Cytiva) or anti-rabbit IgG (NA934, Cytiva).

2.7. Invasion, migration and cell adhesion assays

5% FBS-medium was placed in the lower chamber and used as chemoattractant in both experiments. In the case of invasion, it was assessed in Matrigel (30 μg; 45356231, Corning) coated transwells. 7.5 x 10^4 cells were seeded in the upper chamber in serum-free medium. For migration assessment, 2.5 x 10^4 cells were seeded in serum-free medium in the upper chamber of 48-Well Micro Chemotaxis Chamber (NeuroProbe, AP48). After 24h, invading or migrating cells were fixed with 4% paraformaldehyde and stained with 0.2% crystal violet or fixed and stained using the Kwik Diff kit (Epredia), respecively. Images were taken with an Eclipse TE300 Nikon microscope and quantified using ImageJ. Invasions to evaluate the effect of SGC3027 PRMT7 inhibitor (SML2343, Sigma-Aldrich) were carried out pre-treating cells with 10 μM of inhibitor overnight. Cell adhesion was performed as previously described [11], using pre-covered well with laminin or collagen IV (5 μg/cm^2).

2.8. MTT assay

Cell viability was assessed using the CellTiter 96 Aqueous one solution cell proliferation assay kit (Promega) following manufacturer's protocol as previously described [11]. For assessing the relevance of SGC3027 pharmacological inhibitor in PCa cells, cells were cultured with 10% FBS media with 10 μM (SML2343, Sigma-Aldrich).

2.9. Metastasis assays in chicken embryos

The experiments were performed as described previously [19]. Briefly, 1x10^6 of PC3-Cas9 CTL or PC3-Cas9 *PRMT7* KO1 and KO2 were inoculated into chorioallantoic membranes (CAMs) of embryonic day 10 (E10) chicken embryos. On day 7 (E17) after inoculation, the primary tumors and the bone marrows of the embryos were isolated. Primary tumors were sized and weighted and DNA from bone marrows was extracted using a XNAT2-1 KT kit (Sigma Aldrich). The presence of human Alu sequences within the DNA of the chicken bone marrows was analyzed by qPCR as described before. Primer sequences are listed in the Supplementary Table 1.

2.10. Tumor growth and bone metastasis in nude mice

Mice studies were carried out in strict compliance with the European Community Council Directive (2010/63/EU) and following guidelines for animal research from Complutense University of Madrid (UCM) Ethical Committee, approved by Community of Madrid (Spain) with reference (PROEX 127.0/21). Bone metastasis experiments were carried out as previously described [20]. Briefly, PC3 cell lines, both control and *PRMT7* knock-out, were infected with GFP-Luciferase Lentivirus and sorted. 10^5 cells were injected in the left cardiac ventricle of male NOD SCID J mice (Charles River Laboratories). Mouse metastasis appearance was monitored by IVIS (IVIS Lumina III, Perkin Elmer) after injecting the animals with luciferin (150 mg/kg, Biotherma).

For routine histological analysis, bones were fixed in 10%-buffered formalin (Sigma), decalcified in 0.5 mol/L EDTA for 7 days followed by incubation in 30% sucrose and embedded in paraffin. 2 μm paraffin sections were subjected to immunohistochemical analysis using an antibody against GFP (#2956, CST). Tissue slides were scanned using the AxioScan Z1 scanner (Zeiss). Digital images were analyzed, and the number of micrometastasis was determined in 1 or 2 slides from 4 mice randomly chosen per group. A microscope and software calibration for size measurement was conducted using a TS-M2 stage micrometer (Oplenic Optronics).

2.11. RNA isolation and sequencing

Total RNA from three replicates of *PRMT7*-KO2 and control PC3 CTL cell lines was extracted using NucleoSpin RNA kit (Macherey-Nagel). mRNA quality control checks and NGS sequencing for RNA-seq analysis was performed at NIMgenetics facility (Madrid, Spain). Stranded RNA library preparation was performed using TruSeq mRNA Library Prep (Illumina, Inc) encompassing mRNA capture, fragmentation, cDNA synthesis, adapter ligation, amplification, and purification of the strand-specific libraries. Concentration and profile of libraries was determined using TapeStation (Agilent Technologies), also quantified by fluorimetry with the Qubit system (Thermo Fisher Scientific Inc). Libraries were normalized and pooled in equimolar concentrations for the optimal generation of DNA clusters. Paired-end sequencing (2x100bp) of the previously enriched, indexed and multiplexed libraries was performed using the high-throughput platform NovaSeq 6000 (Illumina Inc), with a read quality of 85%>Q30. To validate the RNA-seq results, reverse transcription (RT) was performed using Superscript IV Reverse Transcriptase (ThermoFisher). Triplicate samples with their corresponding controls were assessed by qPCR, performed at the UCM Genetic and Genomic Facility. Gene fold changes were determined using the $2^{-\Delta\Delta Ct}$ algorithm. All the primer sequences are listed in Supplementary Table 1. GAPDH was used as the reference gene to normalize gene expression.

2.12. RNA-Seq data processing and analysis

RNA-Seq data in FASTQ format were mapped against the reference human genome GRCh38.p13 using STAR v2.7.9a [21] and GENCODE V38 annotation as a gene model that included a total of 60,649 annotated genes (including protein coding and non-protein coding genes, e.g. miRNAs, lncRNAs, …). Gene-level abundances were counted using HTSeq [22], a software which is internally available in STAR. Downstream analyses were performed using R v4.1.2 [23]. Lowly expressed genes were filtered out when accounting for less than 15 read counts across all samples.

2.13. Differential gene expression analysis

Differential expression analysis was carried out using DESeq2 v1.34.0 [22] with the design formula ~ Condition, a factor with two different levels (i.e., g*PRMT7*-KO, gCTL). Genes were considered differentially expressed (DEG) using a 5% FDR and an absolute log2 Fold Change >1 as thresholds.

2.14. Gene ontology overrepresentation analyses

Gene ontology (GO) overrepresentation analysis of biological process terms was performed using the clusterProfiler v4.4.2 [24] and org.Hs.eg.db v3.14.0 [25]. Redundant GO terms were excluded for graphical representation using the rrvgo v1.6.0 [26], that is based in semantic similarity and adjusted p-value.

2.15. TF enrichments

Transcription factor (TF) enrichments were calculated within promoters of DEGs using ReMapEnrich v0.99.0 [27] that compute overlaps between TF binding sites (established in non-redundant peaks ReMap2022 hg38 catalog [27]) and promoter regions. Gene promoters were established at 2500 upstream and 500 downstream base pairs of

the TSS using the GenomicRanges v1.46.1 [28].

2.16. TF activity based on gene expression

The regulatory activities of TFs were estimated per sample from gene expression data by applying the Weighted Mean method of TF-targets of regulons (confidence levels A-C) provided by decoupleR v2.0.1 [29]. Normalized activities were used to calculate the standard deviation of each TF across samples. Ultimately, we utilized standard deviation as a metric to evaluate variation in TFs, we ranked them, and we selected the 50 TFs with the highest values.

2.17. Regulatory network of TFs modulated by PRMTs

Both experimental and public datasets of TFs with methylation sites regulated by PRMTs and their target genes were handled to outline reported interactions underlying cell-adhesion processes. Proteins with methylation sites regulated by PRMTs were collected from the processed methylomes of PRMT4, PRMT5 and PRMT7 [30]. Among all the collected PRMTs proteins, only those listed in top 50 TFs with highest variation in estimated activities described above were selected for network building. Additionally, TFs were classified according to the occurrence of arginine methylation sites in their amino acid sequence using public data from dbPTM database (https://awi.cuhk.edu.cn/dbPTM).

Regulatory interactions between the selected TFs and their target genes were established according to the occurrence of TF binding sites within the promoter of genes annotated to cell adhesion from ChIP-Seq data of ReMap2022 catalog [27]. Once all the interactions were retrieved (PRMT – TF – adhesion gene), the gene network was built and represented using Cytoscape v3.9.1 [31].

2.18. Statistical analysis

The results are expressed as mean value ± SEM of 3–9 independent experiments. Statistical analyses were made by ordinary t-Student tests, Mann-Whitney, one-way ANOVA or two-way ANOVA multiple comparisons test depending on the experiments (p value < 0.05 was considered as significant). GraphPad Prism version 8.4.2 for MacOS X, GraphPad Software (San Diego, California USA, www.graphpad.com), has been used for representing most of the results. Gene ontology (GO) enrichment of CRISPR/Cas9 library screenings was performed using Metascape [32], gene set enrichment analysis (GSEA) and Human Molecular Signatures Database (MSigDB) GO biological process C5 as background [33]. R statistical environment [23] was used for representing some graphs. Venn diagrams were computed using Venny 2.1.0 [34].

2.19. Study approval

Slides of FFPE embedded primary tumor PCa samples were obtained from Hospital Clínico San Carlos Hospital Biobank (Madrid, Spain) in accordance with Institutional Review Board approved protocols. Surgical resection samples of primary tumor (PT) from patients with or without de novo metastatic disease were selected by Dr. Puente Vázquez, Dra. Vidal and analyzed Pathologist Dr. Saiz-Pardo Sanz from Clínico San Carlos Hospital (Madrid, Spain). Samples were classified in two groups according to their metastatic abilities and Gleason score (7 or higher, "High" group, 6 or lower "Low" group). RNA from samples was extracted following manufacturer's instructions (High Pure FFPE RNA Micro Kit, Roche, Switzerland). The low quantity and quality of RNA samples with less than 0,01 μg/μL of RNA and less than 0,1 of 260/230 absorbance ratio were excluded from further analysis. Levels of *PRMT7* gene expression between the "High" and "Low" groups were assessed by RT-qPCR using specific primers listed in Supplementary Table 1 at Genetic and Genomic facility of UCM. Gene fold changes were determined by the $2^{-\Delta\Delta}$Ct algorithm. GAPDH was used as the reference gene to normalize gene expression. Publicly available normalized RNAseqV2 data prostate adenocarcinoma (PRAD) patients from TCGA was downloaded from UALCAN (https://ualcan.path.uab.edu/) [35,36].

3. Results

3.1. CRISPR screenings reveal several genes and biological processes significant for mPCa invasive process

We decided to conduct two unbiased high-throughput CRISPR/Cas9 screenings to identify new essential genes in metastatic castration resistant prostate cancer (mCRPC) using the well stablished cellular models DU145 and PC3. The GeCKO V2 Human CRISPR knockout pooled library, capable of producing the depletion of almost 20,000 genes, by targeting each gene with three differents gRNA, seemed the optimal choice [14]. First, DU145 and PC3 highly metastatic cell lines, with stable Cas9 expression, were generated using a lenti-Cas9 blast construct. Then, DU145-Cas9 and PC3-Cas9 cells were infected with lentivirus containing the gRNA library, using a low infection efficiency (MOI 0.5), to ensure single cell infection. The viral infection led to the introduction of the gRNA construct, containing the puromycin resistance gene, into cells' DNA; therefore, cells were treated with puromycin after the lentiviral infection to remove the cells without gRNA construct.

Next, to distinguish the genes that sustain metastatic abilities of prostate cancer tumor cells, we conducted an invasion assay in a Matrigel-coated Boyden chamber. DNA from cell populations that had lost their invasive abilities, which remained on top of the Matrigel membrane and DNA from the cells that retained them, at the bottom of the membrane, was isolated separately. Subsequently, gRNAs that had been incorporated in the DNA of our cellular models, were amplified by PCR, sequenced, and analyzed using the MAGeCK algorithm [17], as outlined in Fig. 1A.

We were able to identify 990 genes for PC3 and 884 genes for DU145 cell line screenings (Fig. 1B and C and Supplementary Tables 2–3), whose depletion was able to significantly reduce PCa cells invasive capacities. Remarkably, 27 of them were common for both cell lines, which made us hypothesize that those genes could be more general regulators of mCRPC invasion, rather than specific regulators of one mCRPC cell line (Fig. 1D; Supplementary Table 4). Notably, among them, we found genes, such as the N-acetylglucosaminyltransferase V, MGAT5, previously associated to metastatic prostate cancer (mPCa) cell invasiveness [37], proving the efficiency of CRISPR/Cas9 library technology to unbiasedly identify relevant mPCa modulators.

Further, we conducted several gene ontology (GO) biological pathway enrichment analyses to explore whether any biological pathway was enriched in our screenings. GO enrichment analyses of PC3 screening using Metascape [32] revealed that the genes were mainly involved in regulation of metabolism, immune system, cell locomotion and cell adhesion (Fig. 2A; Supplementary Table 5A). The same analysis in the DU145 screening revealed enrichment in pathways such as regulation of proliferation and nucleotide excision repair, regulation of vesicle transport and cytoskeleton reorganization or inorganic ion homeostasis (Fig. 2B; Supplementary Table 5B).

Moreover, gene set enrichment analyses (GSEA) analysis revealed an enrichment in pathways related to epithelial-to-mesenchymal transition (EMT), negative regulation of stem cell proliferation or regulation of protein polyubiquitination, among others for the PC3 cell screening (Fig. 2C; Supplementary Table 5C). Meanwhile for the DU145 screening, GSEA analysis showed an enrichment in mRNA nuclear processing, ion homeostasis or negative regulation of Jun kinase, among others (Fig. 2D; Supplementary Table 5D). Overall, the biological pathways implicated in mCRPC invasion seemed different between both cell lines and depending on the algorithm used, over-representation analysis (ORA) or GSEA, the biological processes varied considerably. The differences in

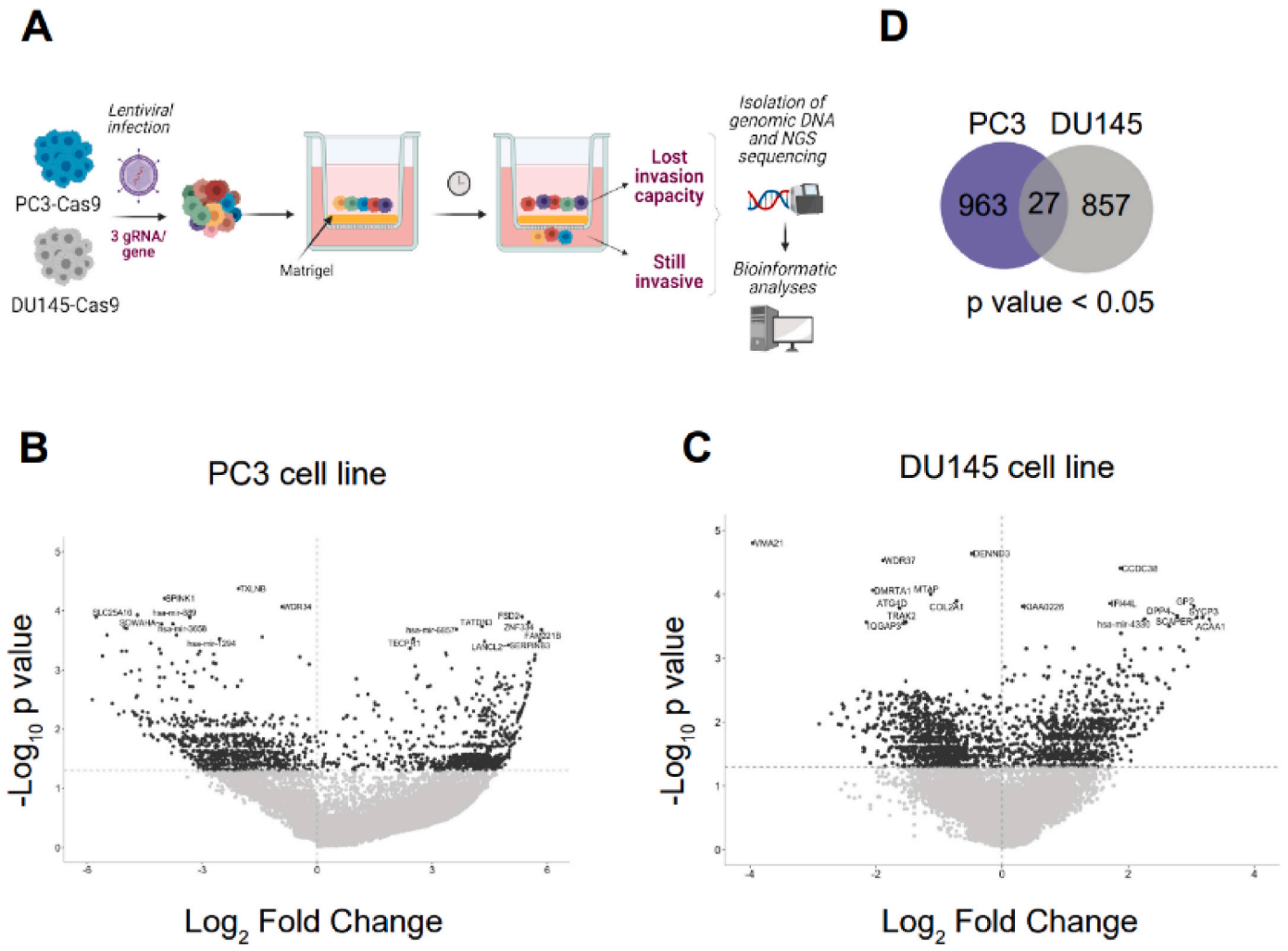

Fig. 1. CRISPR/Cas9 screening experimental design and results. A Graphical scheme of the experimental design of CRISPR/Cas9 screenings. **B** Volcano plot showing PC3 CRISPR/Cas9 screening results. **C** Volcano plot showing DU145 CRISPR/Cas9 screening results. **D** Venn diagram showing the number of genes significantly associated to PCa invasive process in each line and number of common genes between both screenings.

the processes that were enriched in each cell line could be due to the secondary foci where each cell line was isolated from, meanwhile PC3 cell line was isolated from a bone marrow metastasis [38] DU145 cells where isolated from a brain metastasis [39]. Nevertheless, between GSEA significantly enriched biological pathways gene ontology terms, we could find four in common for both cell lines, which were: "regulation of calcium ion transport into cytosol", "multicellular organism process", "DNA modification" and "DNA methylation or demethylation". Additional GO enrichment analyses using Reactome and the molecular signature C5 human molecular classifications, are shown in Supplementary Figs. 1–2.

3.2. *PRMT7 ablation reduces metastatic capacities of mCRPC cell lines in vitro*

To validate the essentiality of the genes whose depletion significantly reduced the invasion capacities of DU145 and PC3 cells in the CRISPR screenings, we selected some of our best hit genes, *TNFSF13*, *MGAT5*, *ZIC5*, *TECPR1*, *PRMT7* and *SYCP3*, based on their association to other types of cancer or metastasis. We studied *in vitro* the ability of PC3 cells to invade in a Matrigel-coated Boyden chamber using fetal bovine serum (FBS) as chemoattractant, after targeting some of our best hits with small interference RNA (siRNA). The downregulation of four of the six candidates selected for validation led to a reduction in the invasive capacity of PC3 cells. However, it was only significant for *PRMT7*, *SYCP3* and *TECPR1* (Fig. 3A). Since *PRMT7* was one of the 27 common genes found in the initial screening (Supplementary Table 4), we decided to further explore its role in mCRPC. Interestingly, PRMT7 belongs to the mammalian family of arginine methyltransferases which are involved in the introduction of methyl groups in the arginines of several proteins. The nine proteins included in the PRMT family can be classified in three subgroups according to the type of methylation that they carry out, symmetrical dimethylation (sDMA), asymmetrical dimethylation (aDMA) or mono-methylation (MMA). PRMT7 is the sole member in the family included in the type III subgroup, because it is mainly involved in introducing MMA in the arginines of proteins, while the other PRMTs establish aDMAs or sDMAs [40].

PRMT7 has been described as an important regulator of breast cancer [41] and non-small cell lung cancer metastasis [42], however, to our knowledge its role in mPCa has not been explored yet. Therefore, we decided to deeper analyze the role of *PRMT7* in PCa metastasis. First, to unequivocally confirm that the effect on invasion was not due to the disruption of any off-target genes, we inhibited *PRMT7* expression by siRNA in both cell lines and confirmed that its silencing strongly decreased, in both cell lines, their invasive properties (Supplementary Figs. 3A–D).

Next, stable PC3 and DU145 CRISPR/Cas9 *PRMT7* knock-out cell lines were generated using novel gRNAs; different from the ones

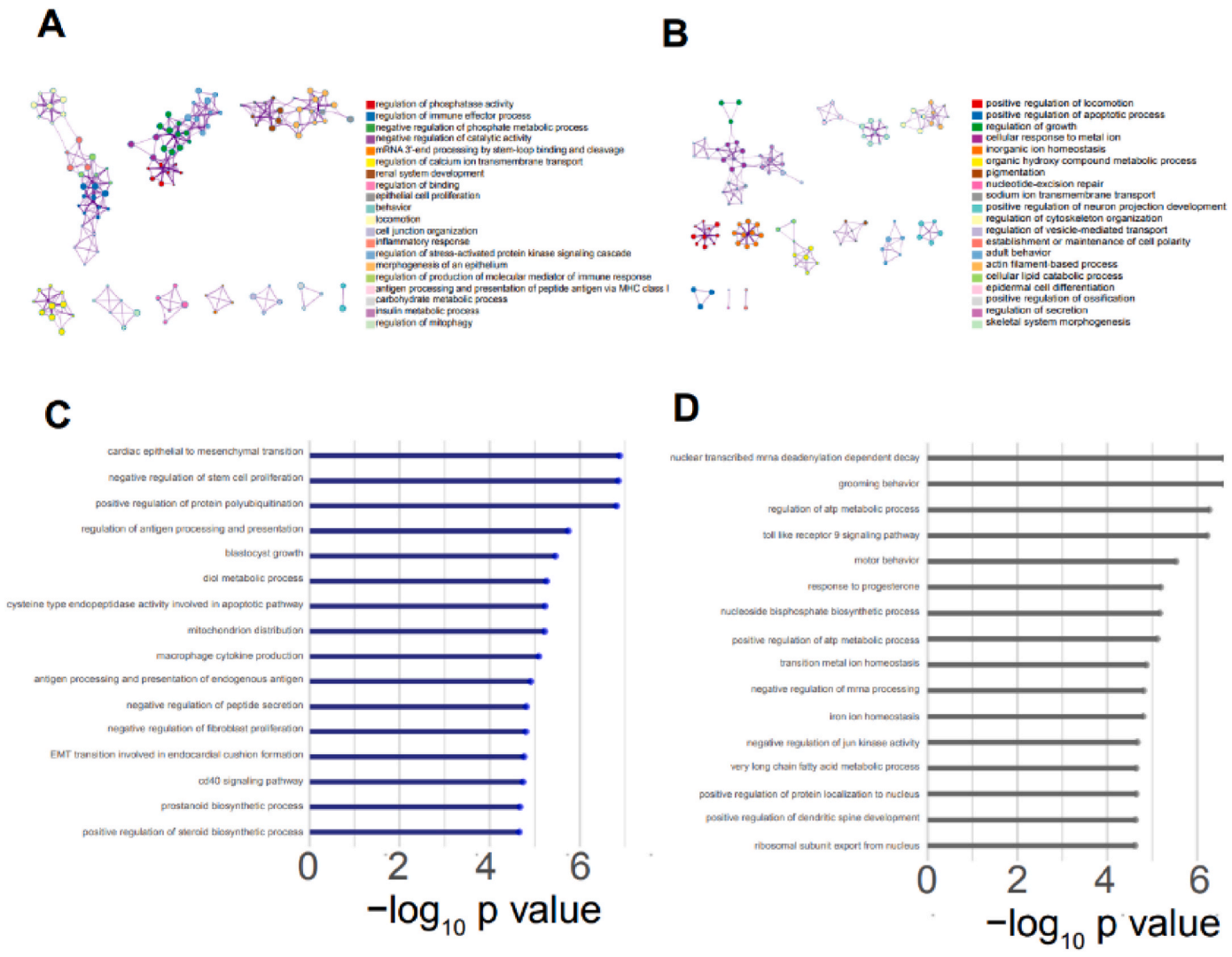

Fig. 2. Biological pathway enrichment analyses of PC3 and DU145 screening results. A-B GO biological pathway enrichment analysis (GO:BP) enrichment analysis using Metascape [32] for **A** PC3 and **B** DU145 screening results. **C-D** Biological pathways GSEA GO enrichment in **C** PC3 and **D** DU145 screening results.

included in the GeCKO CRISPR library [14]. As shown in Fig. 3B and C, western blot analysis confirmed *PRMT7* depletion in PC3 and DU145 cells without decreasing the expression of *PRMT5*, a member of the PRMT family that has been described to be able to methylate several PRMT7 targets [43]. Additionally, we analyzed the levels of MMA observing a reduction in the *PRMT7* depleted cells, especially around 78 KDa band (Fig. 3D and E).

Subsequently, we conducted invasion assays using Matrigel-coated Boyden chambers using FBS as chemoattractant for PC3 (Fig. 3F) and DU145 (Fig. 3G) cell lines, validating our initial screening results. We wondered then, if *PRMT7* depletion could either be influencing the ability of cells to degrade the Matrigel used in the invasion assay, or it was also altering cell motility. To differentiate both effects, we conducted a migration assay in an uncoated Boyden chamber using FBS as chemoattractant, observing that *PRMT7* depleted cells had significantly less ability to migrate than their respective controls (Fig. 3H and I) thus suggesting that *PRMT7* regulates mPCa cells' migration.

Previous studies have linked *PRMT7* and proliferation in cancer cells [44], so we decided to study the effect of *PRMT7* depletion in mCRPC cell lines viability by performing a MTT assay. As shown in Fig. 3J–K, a significant decrease in viability ratio was observed in *PRMT7* depleted cells, especially at 96h, in comparison to control cells. Hence, these results indicate that *PRMT7* silencing or depletion produces a significant reduction in PC3 and DU145 metastatic abilities in invasion, migration, and viability.

3.3. *In vivo model assays show reduced disseminative capacities of PRMT7 depleted cells*

PRMT7 has been previously implicated in breast cancer metastasis [41] and non-small cell lung cancer [42] progression. Considering these studies and together with our *in vitro* results, we wondered whether *PRMT7* depletion played a role in PCa distant organ colonization in animal models. To this end, we took advantage of the highly metastatic potential of the well-established PC3 cell line, and we performed two different experimental metastasis assays.

First, we conducted a chorioallantoic membrane assay (CAM) [19] as depicted in Fig. 4A. PC3-Cas9 *PRMT7* depleted, and control cells were inoculated separately in the CAM of chicken embryos. Seven days later, primary tumors and bone marrow of chicken embryos were isolated. As shown in Fig. 4B and C, PC3 *PRMT7* depleted cells generated significantly smaller (Fig. 4B) and lighter (Fig. 4C) tumors than control cells. These differences in primary tumor growth *in ovo* agree with the decreased viability observed *in vitro*. Moreover, since PC3 cells display bone marrow tropism [20], disseminative properties of tumor cells were assessed amplifying by qPCR human Alu sequences (not present in

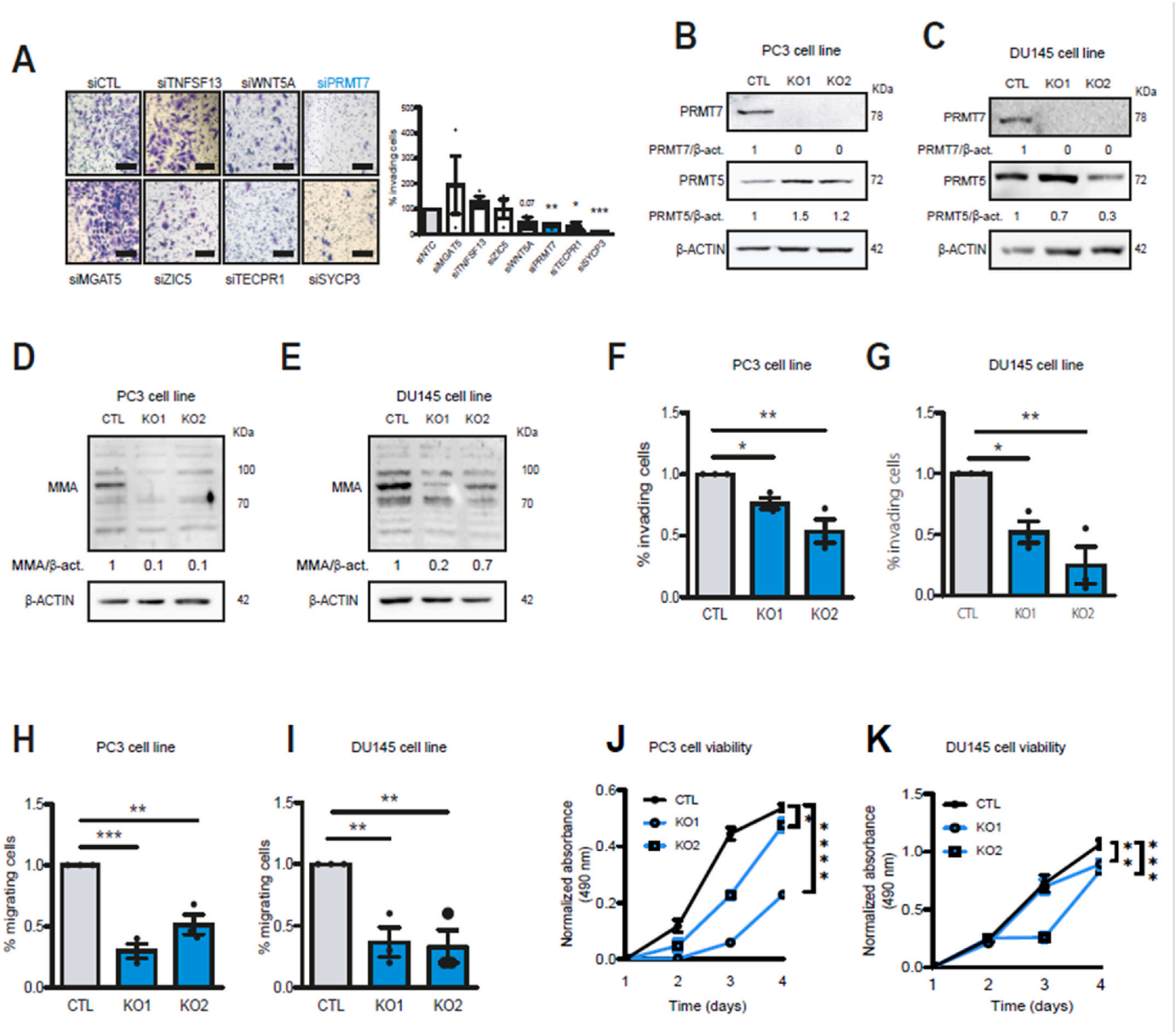

Fig. 3. Validation of our best hits by siRNA technology and further *PRMT7* role in mPCa study by CRISPR/Cas9. A Invasion assay of PC3 inhibited cells using specific siRNA to target our best gene candidates versus control (siCTL) cells. **B–C** Representative western blot of PRMT7, PRMT5 and β-actin protein levels in **B** PC3-Cas9 and **C** DU145-Cas9 cell lines. The numbers below each lane represent PRMT7/β-actin or PRMT5/β-actin densitometric quantification referred to control cells (n = 3). **D-E** Representative western blot of MMA and β-actin protein levels in **D** PC3-Cas9 and **E** DU145-Cas9 cell lines. The numbers below each lane represent MMA/β-actin densitometric quantification referred to control cells (n = 3). **F-G** Invasion assay of *PRMT7* depleted versus control (CTL) cells of **F** PC3-Cas9 and **G** DU145-Cas9 cell lines (mean ± SEM of n = 3 biological replicates, by unpaired Student's *t*-test *P < 0.05, **P < 0.01, ***P < 0.001). **H–I** Migration assay of *PRMT7* depleted versus CTL cells of **F** PC3-Cas9 and **G** DU145-Cas9 cell lines (mean ± SEM of n = 3 biological replicates, by unpaired Student's *t*-test *p < 0.05, **p < 0.01, ***p < 0.001). **J-K** Viability assay of *PRMT7* depleted versus CTL cells of **J** PC3-Cas9 and **K** DU145-Cas9 cell lines (mean ± SEM of n = 9 biological replicates, by TWO-way ANOVA *p < 0.05, **p < 0.01, ***p < 0.001, ****p < 0.0001).

chicken DNA) in the samples from chicken bone marrow. Less percentage of human Alu sequences were detected in chicken embryos inoculated with PC3 *PRMT7* depleted cells than in embryos inoculated with control cells, which indicates that *PRMT7* depleted cells showed a lower capacity to disseminate from the primary tumor to the bone marrow of chicken embryos than control cells (Fig. 4D).

Previous studies showed that upon direct inoculation of PC3 cells in the blood circulation of immunodeficient mice (NOD-SCID), they were able to generate metastatic foci in distant tissues including femur and tibia, jaws, and ribs [20]. Hence, we decided to inoculate control and *PRMT7* depleted PC3 cells engineered to express a luciferase-GFP DNA construct, using a lentiviral approach. They were inoculated in the left cardiac ventricle of athymic nude mice, as previously described [46]. Mice were analyzed using an IVIS system and were sacrificed after 28 days, and their tissues (including femur, tibiae, and sternum) were harvested, fixed, and analyzed for the presence of micrometastatic foci as depicted in Fig. 4E. We found distant metastasis in 50% of mice inoculated with control cells in comparison to 12% or 33% of mice inoculated with *PRMT7*-KO1 and *PRMT7*-KO2 depleted PC3 cells, respectively. A representative picture is shown in Fig. 4F. Unexpectedly, several macrometastases detected displayed visceral localization, while no bone macrometastases were detected (Supplementary Fig. 4). To analyze the presence of micrometastases of PC3 cells in bone marrow inmunohistochemistry assays of bone marrow from tibia, femur and

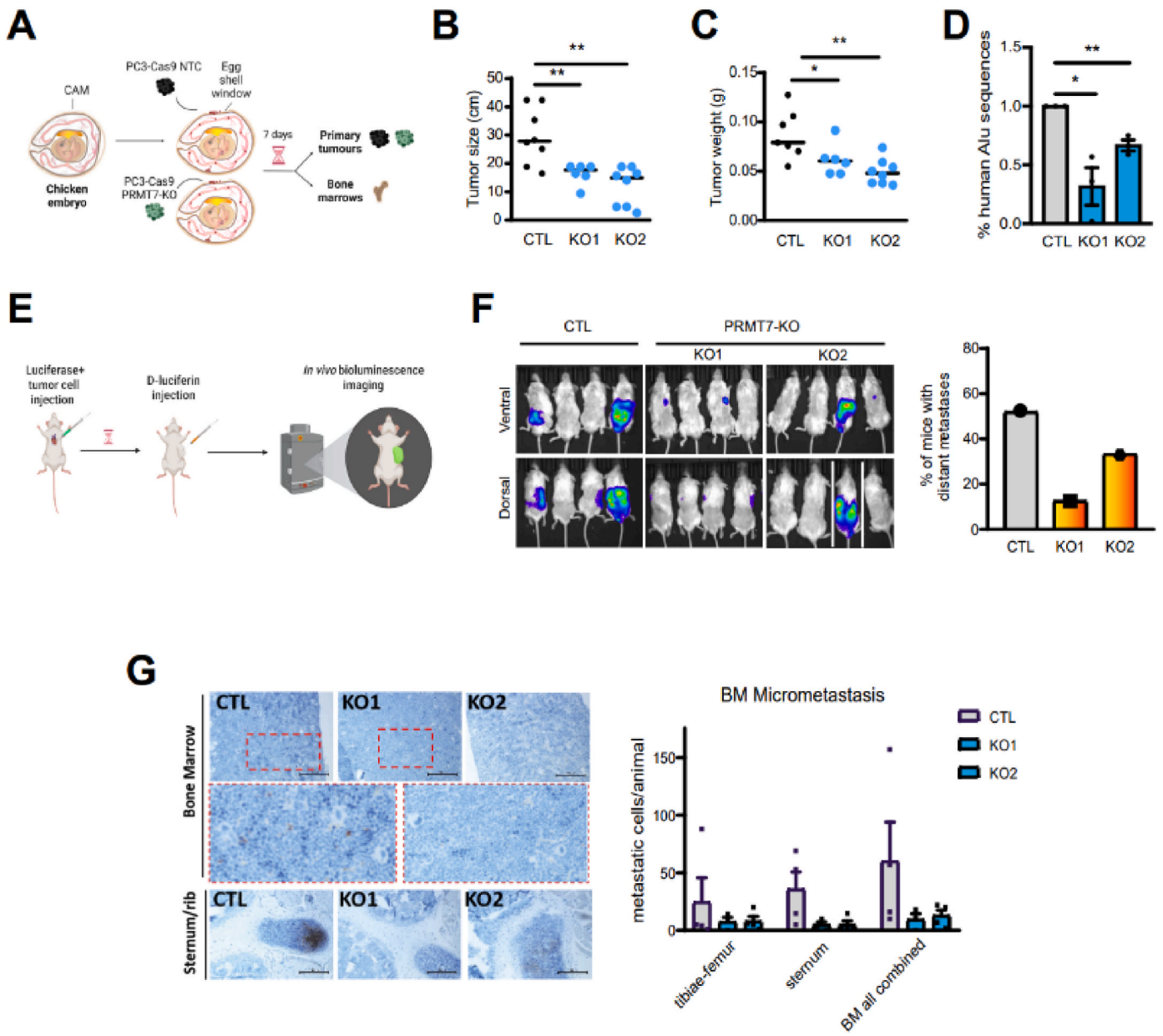

Fig. 4. ***PRMT7*** **depletion reduces proliferative and disseminative abilities of PCa cells** ***in ovo*** **and** ***in vivo*****. A** Graphical scheme of *in ovo* studies experimental design. **B–C** Graphs representing primary tumor **B** size and **C** weight (mean ± SEM of n = 6–8 inoculated chicken embryos, by ordinary ONE-way ANOVA *p < 0.05, **p < 0.01, ***p < 0.001). **D** Graph representing percentage of human Alu sequences amplified by qPCR in chicken bone marrow (mean ± SEM of n = 3, by Student's *t*-test). **E** Graphical scheme of *in vivo* dissemination assay experimental design. **F** Left panel, representative pictures of metastases generated by CTL, *PRMT7*-KO cells. Right panel shows the percentage of mice with distant metastasis (n = 12). **G** Left panel are representative pictures of immunohistochemistry of GFP positive cells in the mice bones. Right panels show the percentage of disseminated tumor cells (DTC) in mice bone marrow (mean ± SEM of n = 9 animals per group, by Student's *t*-test).

sternum were performed. Quantification of disseminated tumor cells by GFP staining detection revealed that *PRMT7* depletion in PC3 cells severely reduced the formation of bone marrow micrometastases compared to PC3 control cells (Fig. 4G). Consequently, these results highlight the relevance of PRMT7 in controlling biological processes that are directly implicated in the PCa metastasis onset both *in vitro* and *in vivo*.

3.4. Expression of relevant cell adhesion molecules is regulated by PRMT7

To elucidate the biological mechanisms controlled by PRMT7 that facilitate distant organ colonization of primary tumor PCa cells, we decided to conduct a differential expression analysis (DEG) of PC3 *PRMT7* depleted versus control cells. Out of the total genes analyzed, gene expression of 781 genes was significantly altered (Fig. 5A; Supplementary Table 6). Among the most differentially expressed genes we found the phospholipase *PNPLA4*, the histone binding protein *SFMBT2* and several genes related to cell adhesion such as *TUBAC3* or *CHST15*. *TUBAC3* encodes a protein implicated in microtubule formation, meanwhile *CHST15* encodes a glycosaminoglycan that binds to proteins to generate proteoglycans, important components of extracellular matrix.

Consecutively, a GO over-representation analysis was performed as shown in Fig. 5B, which revealed that cell-substrate adhesion term was over-represented. Hence, we explored in more depth the overall expression of genes annotated to the cell adhesion parental ontology

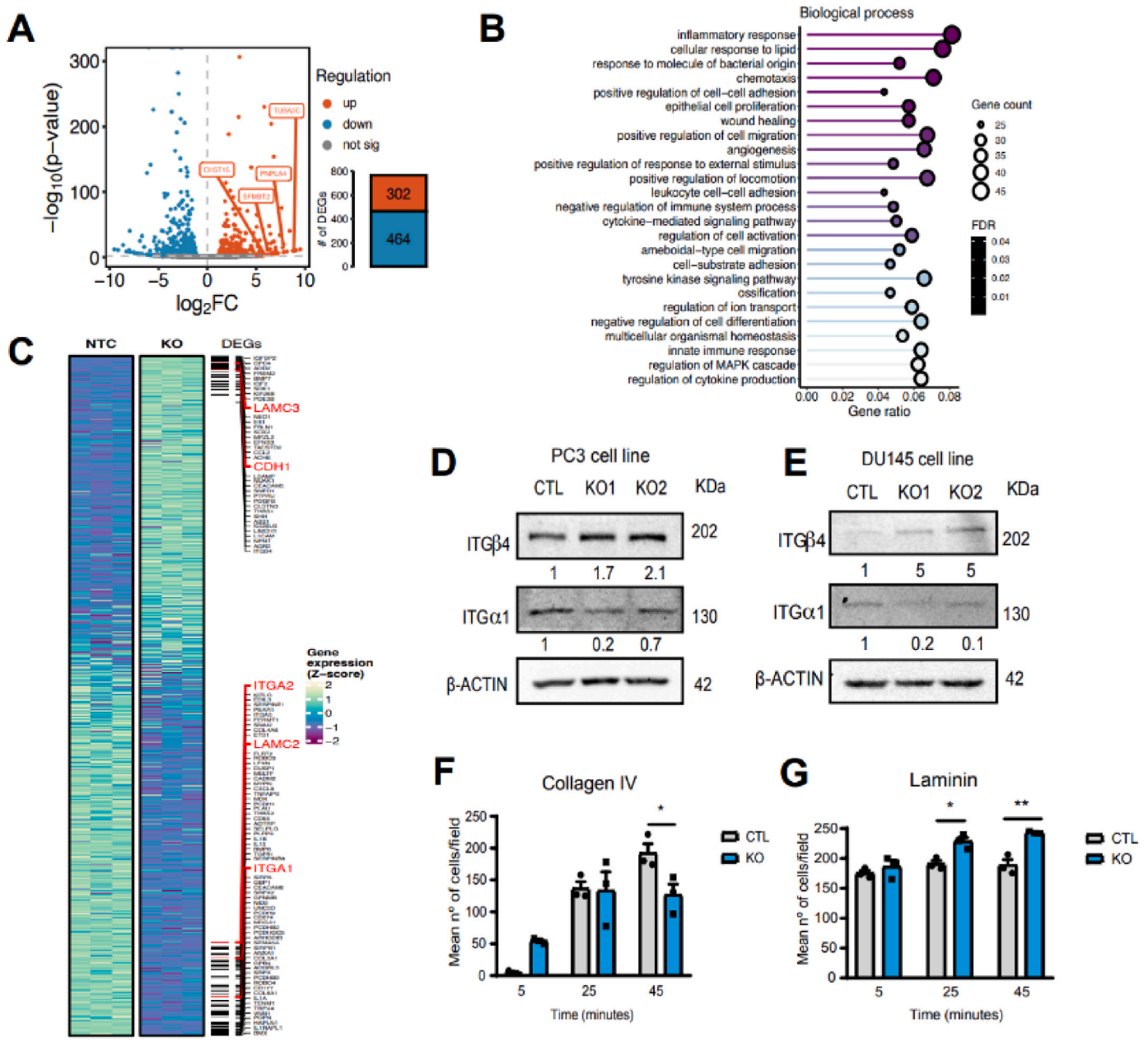

Fig. 5. *PRMT7* depletion leads to an adhesion molecule switch in PC3 cells. A Volcano plot showing differentially expressed genes (DEGs) (adjusted p-value <0.05, $|\log FC| > 1$) from the differential gene expression analysis of PC3 control versus *PRMT7* depleted cells and a barplot representing the number of genes that significantly changed their expression, accounting for the number of genes that were upregulated (red) and downregulated (blue) in *PRMT7* depleted cells. **B** Over-representation analysis of biological process GO terms in DEGs (adjusted p-value <0.05, $|\log FC| > 1$) of *PRMT7* depleted cells compared to control cells, representing top 25 terms with highest gene ratio with an adjusted p-value cutoff of 0.05 and redundant GO terms removed. **C** Heatmap showing the gene expression (Z-score) of the genes found in parental GO term cell adhesion sorted by $\log_2$ fold change. Horizontal lines denote DEG positions, and those of interest are highlighted in red. **D-E** Western blot analysis of ITGα1 and ITGβ4 protein levels in **D** PC3-Cas9 **E** DU145-Cas9 cells. The numbers below each lane represent ITGα1/β-actin or ITGβ4/β-actin respectively densitometric quantification referred to control cells. **F-G** Graph representing mean number of cells per field adhered to **F** collagen IV or **G** laminin (mean ± SEM of n = 3, by unpaired Student's *t*-test *P < 0.05, **P > 0.01).

term (GO:0007155) (Fig. 5C). Surprisingly, we observed that some genes such as *CDH1* or *LAMC3*, were upregulated in the *PRMT7* depleted cells, while others such as *ITGA1, ITGA2* or *LAMC2* were downregulated.

To validate our RNA-seq results, we randomly selected some of the genes included in the cell adhesion group and analyzed its expression in independent PC3 *PRMT7* depleted and control samples by RT-qPCR, as shown in Supplementary Fig. 5. Cell adhesion has been described as a crucial biological process mediating motility of cells and colonization of distant organs, being integrin receptors especially relevant [47]. Moreover, the overexpression of some integrins has been associated with bad prognosis in several cancers and depending on the type of integrin expressed on their membrane, cells can adhere better to specific types of extracellular matrixes [48]. Thus, we analyzed the protein levels of ITGα1 and ITGβ4 that, respectively, mediate the binding to collagen IV or laminin matrixes.

Western blot analyses revealed that ITGα1 protein levels were significatively reduced in *PRMT7* depleted cells, meanwhile ITGβ4 protein levels were significatively increased in comparison to control cells, in both cell lines, PC3 (Fig. 5D) and DU145 (Fig. 5E). ITGα1 mediates the binding of cells to collagen type IV and ITGβ4 to laminin present in the

extracellular matrix. Interestingly, overexpression of exogenous *PRMT7* [49] reduces ITGβ4 levels in both control and *PRMT7* depleted cells and increases ITGα1 levels, which agrees with previous results (Supplementary Fig. 6). Hence, cell adhesion to collagen IV (Fig. 5F) and laminin (Fig. 5G) was evaluated, observing a change in the selective adhesion to these matrixes. Overall PC3 cells, both *PRMT7* depleted and control cells, had more ability to adhere to laminin than to collagen IV. However, we observed at longer time points that control cells preferentially adhered to collagen IV, while *PRMT7* depleted cells maintained a better adhesion to laminin. These results indicate that overexpression of *PRMT7* in primary tumor cells could be producing a switch in the expression of cell adhesion molecules leading to a reduced cell adhesion to the extracellular matrix together with an increase motility, promoting dissemination to distant organs.

3.5. Arginine methyltransferase 7 regulates the activity multiple transcription factors

PRMT7 is present in the nucleus and cytoplasm introducing post-transcriptional modifications in several proteins [43]. Hence, we wondered how PRMT7 modulates the expression of the cell adhesion genes identified in the transcriptomic analysis. Accordingly, we investigated which transcription factors (TFs) might be regulating these transcriptome differences using two alternative approaches. First, we performed an enrichment analysis of TF binding sites within promoters of differentially expressed genes in PC3 cells that revealed several TF related to Polycomb complex-2, such as EZH2 (Fig. 6A). Indeed, this histone methyltransferase had already been associated with PCa progression [9].

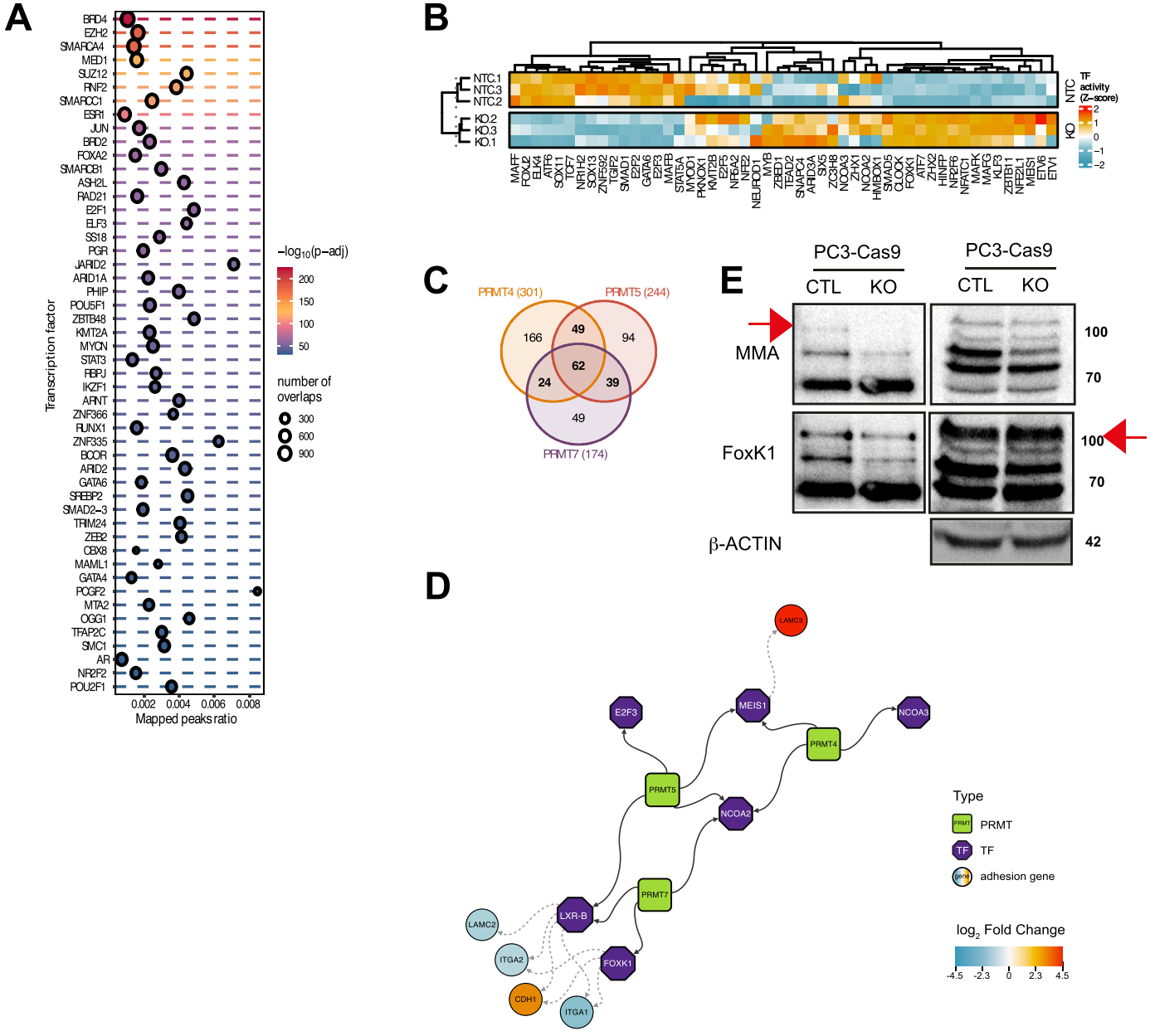

Fig. 6. PRMT7 drives cell adhesion molecule reprogramming through several TF methylation. A Top 50 most significant enriched TFs in the promoter regions of differentially expressed genes (DEGs). **B** Heatmap showing TF activity estimated from TF regulons expression, representing the top 50 most variable TFs across CTL and *PRMT7* depleted cell samples. **C** Venn diagram of the target proteins of PRMT7, PRMT4 and PRMT5 described in Li et al.[30]. **D** Regulatory network of transcription factors (purple hexagons) that are methylated by PRMT7, PRMT4 and PRMT5 (green squares), and can bind to cell adhesion gene promoters (circles). **E** Western blot analysis of MMA and FoxK1 levels after FoxK1 immunoprecipitation (left) and MMA, FoxK1 and β-actin levels in input (right). Red arrows show FoxK1 protein band.

Alternatively, we also inferred the regulatory activities of TFs based on the expression values of their target genes. From these estimated activities, we calculated the standard deviation of each TF, and selected the top 50 TFs that exhibited the highest variation across samples, independently of their experimental treatment. Our results revealed that the most variable TFs show a high concordance with changes in TF activity between *PRMT7* depleted and control cells. Surprisingly, we identified 7 of top 50 TFs with arginine methylation sites from dbPTM database, and intriguingly 6 of them presented a robust increased activity on PRMT7 depleted samples (Fig. 6B). Curiously, we found that 4 of those 7 TFs (FoxK1, LXR-β codified by *NR1H2* gene, NCOA2 and NCOA3) were PRMT7s targets as described in the recently published PRMT4, PRMT5 and PRMT7 methylomes [30]. In Fig. 6C is depicted a Venn diagram showing the proteins susceptible of being methylated by the three, two or one of the PRMTs. Therefore, we focused our analysis on the TFs controlling the expression of cell adhesion related genes susceptible of being methylated by PRMT7. FoxK1, LXR-β and NCOA2/3 are the only TF susceptible of being methylated specifically by PRMT7 [30], and able to bind to the promoter of cell adhesion genes, including the analyzed promoter of E-cadherin, *CDH1* and integrins α1 and α2, *ITGA1/2*, where they could promote or inhibit their expression, as summarized in Fig. 6D and Supplementary Fig. 6. Moreover, we demonstrate here that PC3 *PRMT7*-KO cells present lower levels of mono-methylated FoxK1 as shown in Fig. 6E and that the

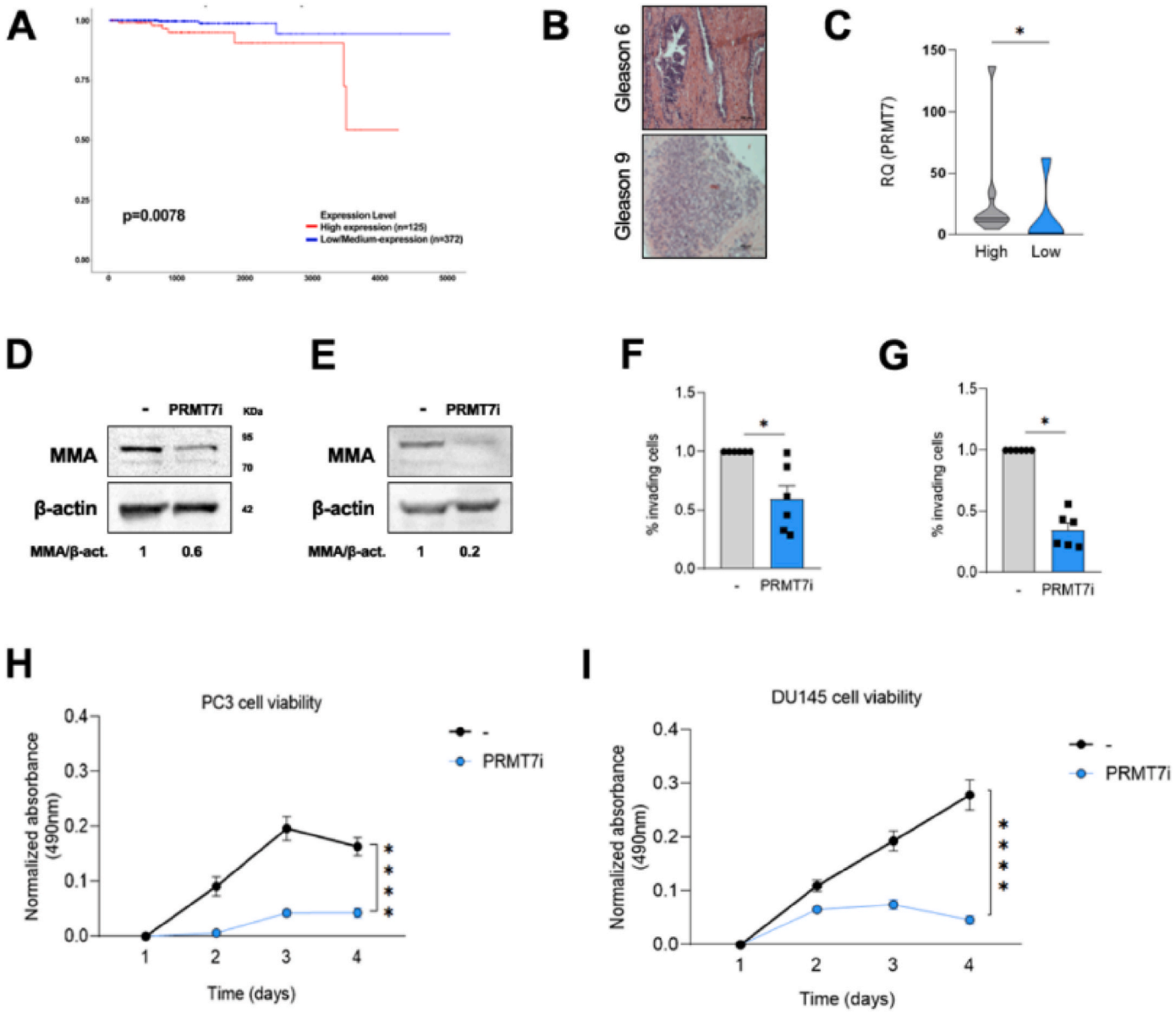

Fig. 7. PRMT7 clinical approach. A Kaplan-Meier curve showing the overall survival rate of TCGA prostate cancer patients' cohort (TCGA-PRAD) with high versus low/medium *PRMT7* expression levels. **B** Representative hematoxylin and eosin stainings of Hospital Clínico San Carlos PCa primary tumor samples of showing the aggressivity of tumors measured by Gleason score *PRMT7* (Scale bars: 50 μM). **C** *PRMT7* gene expression levels in PCa primary tumor samples with higher (n = 8) versus lower (n = 5) Gleason score samples (mean ± SEM of n = 13 primary tumor samples, by unpaired Mann-Whitney test *p < 0.05, **p < 0.01, ***p < 0.001). **D, E** Representative western blot of Arginine monomethylation (MMA) levels in **D** PC3 and **E** DU145 cells upon treatment with 10 μM of SGC3027 (PRMT7 inhibitor). The numbers below each lane represent MMA/β-actin densitometric quantification referred to control cells. **F-G** Invasion assay of PRMT7 inhibited versus vehicle cells of **F** PC3 and **G** DU145 cell lines (mean ± SEM of n = 6 biological replicates, by unpaired Student's *t*-test *p < 0.05, **p < 0.01, ***p < 0.001). **H–I** Cell viability assay of PRMT7 inhibited versus vehicle cells of **H** PC3 and **I** DU145 cell lines (mean ± SEM of n = 9 biological replicates, by TWO-way ANOVA *p < 0.05, **p < 0.01, ***p < 0.001, ****p < 0.0001).

downregulation of *FOXK1* and/or *NR1H2* genes leads to a significant reduction in the invasive capacities of PC3 cells, reproducing the phenotype observed when *PRMT7* is depleted in the same cells (Supplementary Figs. 7A–C). Altogether these results suggest that *PRMT7* depletion alters the activity of relevant transcription factors such as FoxK1, LXR-β and NCOA2/3 that would reprogram the type of cell adhesion molecules expressed on cell surface.

3.6. Potential use of PRMT7 as a new therapeutic target or biomarker

To further explore the role of *PRMT7* in PCa metastasis, the TCGA gene expression data of PCa patients was retrieved from UALCAN database. As shown in Fig. 7A, the overall survival rate of patients with higher *PRMT7* expression was significantly reduced. Additionally, we also explored *PRMT7* expression by Gleason score (GS) groups in these samples, observing a significant upregulation from GS 6 and above compared to healthy samples (Supplementary Fig. 8). Moreover, we validated this result in a cohort of FFPE-embedded PCa primary tumor samples recruited from Hospital Clínico San Carlos (Madrid, Spain). Tumor samples were divided into two groups according to their aggressiveness and the diagnosis of metastasis in the patient. In the group labeled as Low, tumor samples with a GS of 6 and no metastasis present in patients were included, meanwhile samples with a GS equal or greater than 7 and diagnosis of metastasis were included in the group labeled as High. Supplementary Table 1 summarizes characteristics of patients included in the study, and Fig. 7B shows representative H&E staining images of tumors of both groups. As shown in Fig. 7C, the samples classified as High showed higher *PRMT7* expression levels than Low group. These results suggest that *PRMT7* may be a potential biomarker of PCa malignancy.

Because some inhibitors of the PRMT family are already in clinical trials [50] and PRMT7 inhibitors were already available commercially but have not been tested to prevent or cure mPCa, we wanted to study their effectiveness on depleting metastatic abilities of mCRPC. First, we confirmed that the inhibitor reduced PRMT7 activity by analyzing the MMA levels in cells, observing a reduction of them in both treated cell lines compared to cells treated with vehicle (Fig. 7D and E). Next step we studied whether pharmacological inhibition was sufficient to reduce the invasive capacity of mCRPC cell lines. As shown in Fig. 7F and G, PRMT7 inhibitor was sufficient to significantly decrease PC3 (Fig. 7F) and DU145 (Fig. 7G) invasive abilities compared to control cells. Moreover, we observed a reduction in proliferation and/or viability after treating cells with the inhibitor, mainly at 96h (Fig. 7H and I). Altogether, these results suggest that pharmacological PRMT7 inhibition could be an effective approach to decrease the metastatic capacity of PCa cells *in vitro* and open a field of research in *in vivo* and preclinical studies.

4. Discussion

Metastasis in PCa is a complex phenomenon involving many biochemical processes that are largely unknown [51]. Although there are several effective therapies at the initial stages of PCa disease, metastatic castration resistant prostate cancer (mCRPC) has no cure yet. The high incidence of this neoplasia highlights the need for the identification of new targets to be used as prognostic biomarkers and/or therapeutic targets. To our knowledge, our report presents the first two independent large-scale screenings specifically designed for uncovering PCa essential invasion genes using CRISPR/Cas9 based technology in mCRPC. The bioinformatic analysis carried out allowed us to identify many novel genes and biological pathways essential for PCa cell invasive abilities.

Our extended *in vitro* and *in vivo* characterization of *PRMT7* unveils this gene as a critical regulator of PCa tumor progression, being relevant not only for the viability of the metastatic cells but also being able to regulate invasive and migratory ability of cells, which are key to metastasis development. According to our results, PRMT7 controls mCRPC cell viability *in vitro* and *in vivo*. However, the viability reduction upon *PRMT7* depletion would not explain the decrease in PC3 and DU145 motility, as differences in migration and invasion were measured at 24h, while significant viability differences were observed at longer time frames. Moreover, PRMT7 pharmacological inhibition could reduce the viability of other mPCa cellular models, such as LNCaP cells, which are responsive to androgen castration therapies and other types of cancer cells as demonstrated by Wen Liu laboratory [30].

PRMT7 is the only member of the arginine methyltransferase family that belongs to subgroup III and is involved in introducing preferentially MMA [43]. In the context of breast cancer, PRMT7 has been described to methylate E-cadherin proximal promoter, inducing EMT transition [41] and to upregulate the expression of matrix metalloproteinase-9 (MMP9) [52] which all together lead to the progression of the disease. Regarding non-small cell lung cancer, PRMT7 contributes to metastasis appearance through the interaction with HSPA5 and EEF2 [42]. In addition, it has been described that in renal cell carcinoma, PRMT7 can methylate β-catenin promoting its stabilization and the induction of c-myc expression, which is an important regulator of cell proliferation and tumor progression [44]. Moreover, PRMT7 has been described to methylate the Wnt signaling molecule Dishevelled 3 [53], the transcription factor C/EBP-β [54], RNA splicing factor hnRNPA1 [30], suggesting that it, directly or indirectly, could be implicated in several cellular pathways both, in cellular homeostasis and disease. Therefore, due to the high number of biological processes susceptible of being modulated by PRMT7 methylation, we decided to conduct a differential transcriptomic analysis in our mCRPC cellular models, to elucidate the most important processes regulated by PRMT7 which are crucial in the progression of prostate cancer progression. Results showed differences in *CDH1* expression, as expected. However, we did not detect significant changes in other genes like *MMP9*, *HSPA5*, *EEF2, CTNNB1*, nor *MYC* gene expression. We neither observed an enrichment in mRNA transcription nor splicing pathways between our DEG genes. Remarkably, we observed and enrichment of several cell adhesion biological processes. Therefore, we focused our efforts in studying the role of PRMT7 in metastatic prostate cancer cell adhesion which had not been described before.

Cell adhesion to other cells and substrates is a widely known mechanism that contributes to tumor cell migration and invasion ability. In fact, the change in expression of some integrin and laminin receptors, which are a type of well characterized cell adhesion molecules, are already considered malignant biomarkers. For example, alpha 1 subunit of integrin receptors (*ITGA1)* is a pre-malignant biomarker that promotes therapy resistance and metastatic potential in pancreatic cancer [55] while laminin subunit gamma 2 (LAMC2), has previously been identified as a specific marker for metastatic abilities in lung adenocarcinoma [56]. Therefore, our functional validation was focused on demonstrating that *PRMT7* depletion reprograms the type of cell adhesion molecules expressed by tumor cells, and at least validated *ITGA1*, *ITGB4*, *LAMC2*, *LAMC3* and *CDH1*. Additionally, here it is demonstrated that the selective adherence of PC3 cells to different types of extracellular matrixes, such as collagen IV and laminin, is altered because of a cell adhesion protein switch. Interestingly, bone marrow, where 70% of mPCa is found [57], is an organ rich in collagen IV [58]. Therefore, we hypothesize that the upregulation of *PRMT7* expression levels in PCa cells could enhance adhesion to collagen IV rich bone marrow promoting cell survival and metastasis appearance.

In this study, TF activity analysis uncovered a new role for PRMT7 as regulator of several TFs. These results together with already published PRMT7 methylome [30], where FoxK1, LXR-β and NCOA2/3 are found as PRMT7 methylation targets, suggests that arginine methyltransferase 7 could regulate their transcriptional activity in mCRPC cells. Remarkably, FoxK1, a TF susceptible of being methylated by PRMT7 on R161 and R191 residues, is a known regulator of the expression of several adhesion molecules and it has previously been involved in the acquisition mPCa abilities [59,60]. In addition, LXR-β is susceptible of being methylated on R126 and is known to regulate the expression of *LAMC2*

and *CDH157* [61]. Arginine methylation stabilizes E2F1 [62], so we speculate that it may have a similar effect on FoxK1, LXR-β or NCOA2/3 allowing primary PCa cells to gain migratory and invasive abilities as well as improving survival of already established metastatic cells, enhancing the distant organ colonization. Regulation of cellular adhesion molecules via PRMT7-FoxK1/LXR-β/NCOA2/3 may explain the acquisition of migratory abilities showed by the PCa cellular models' studies.

Regarding the use of *PRMT7* as prognostic biomarker or therapeutic target, although further validation analyses with cohorts of a higher sample size are needed, our results are in agreement with the already published analyses conducted by Grypari and collaborators, using TCGA data and Gene Expression Omnibus (GEO) database (GSE21034), point out *PRMT7* as a poor prognosis biomarker for PCa progression. Moreover, Grypari and colaborators also showed a correlation of PRMT7 protein levels with more advanced disease stages by immunohistochemistry [63]. Our work also points out PRMT7 inhibitor as a good therapeutic approach to reduce proliferative but also invasive and migratory capacities of mCRPC cell lines. Indeed, PRMT1 and PRMT5 inhibitors are currently under phase I or II clinical trial studies, respectively (NCT04676516, NCT03573310, NCT05094336, NCT03854227, NCT04089449, NCT03886831, NCT05275478, NCT04794699, NCT05245500). Although we believe PRMT1 or PRMT5 pharmacological inhibitors could be useful in mPCa treatment, our initial screenings did not point out PRMT1 neither PRMT5 as essential regulators of mCRPC, in fact, our Fig. 3B and C prove that PRMT7 depletion without altering the expression of PRMT5, is enough to reduce metastatic abilities of PC3 and DU145 mCRPC cell lines. Hence this work supports PRMT7 as a good pharmacological target for mPCa.

5. Conclusions

In summary, we conducted two independent large-scale CRISPR/Cas9 library screenings with the aim of identifying the essential genes in mCRPC cell invasion and validated some of the most robust gene candidates, being *PRMT7* our best hit. Here, we showed that its inhibition by siRNA or pharmacological approaches or its depletion by CRISPR/Cas9, significantly reduces invasion, migration and viability of mPCa cell lines *in vitro* and viability and disseminative capacities *in vivo*. Further, we have found that its expression is significantly correlated with tumor aggressiveness and a poor overall PCa patient survival. Last, our transcriptomic analysis points out that mechanistically PRMT7 switches the expression of certain adhesion molecules through at least FoxK1 and/or LXR-β methylation, which leads to a change in the adhesion capacity of cells promoting cell migration and invasion. Taking all these results together, we highlight *PRMT7* as a promising biomarker candidate of poor prognosis and a potential new therapeutic target for the treatment of PCa metastasis.

Funding

This work was funded by Comunidad de Madrid under projects 2017-T1/BMD-5468 and 2021-5A/BMD-20956; Grants (PID2020-117650RA-I00 (AGU), PID2019-104143RB-C22 (AP), PID2019-104991RB-I00 (PB) and PID2021-122797OB-I00 (MM)) funded by MCIN/AEI/10.13039/501100011033 and by "ERDF A way of making Europe"; and ARP and AVN have been supported and granted by the Regional Programme of Research and Technological Innovation for Young Doctors UCM-CAM (PR65/19–22460).

Data and materials availability

Results are available in the main text or the supplementary materials. Raw data of CRISPR screenings and RNA-seq are available at ENA archive under request.

CRediT authorship contribution statement

Maria Rodrigo-Faus: Writing – review & editing, Writing – original draft, Visualization, Validation, Methodology, Investigation, Formal analysis, Data curation, Conceptualization. **Africa Vincelle-Nieto:** Writing – original draft, Visualization, Software, Methodology, Formal analysis. **Natalia Vidal:** Resources. **Javier Puente:** Resources. **Melchor Saiz-Pardo:** Resources, Investigation. **Alejandra Lopez-Garcia:** Resources, Methodology, Investigation. **Marina Mendiburu-Eliçabe:** Visualization, Formal analysis, Data curation. **Nerea Palao:** Visualization, Conceptualization. **Cristina Baquero:** Methodology. **Paula Linzoain-Agos:** Investigation, Methodology, Writing – review & editing. **Angel M. Cuesta:** Visualization, Methodology. **Hui-Qi Qu:** Visualization, Methodology, Formal analysis, Data curation. **Hakon Hakonarson:** Supervision, Conceptualization. **Monica Musteanu:** Validation, Supervision, Resources, Methodology. **Armando Reyes-Palomares:** Writing – review & editing, Visualization, Validation, Methodology, Formal analysis, Data curation, Conceptualization. **Almudena Porras:** Writing – review & editing, Supervision, Conceptualization. **Paloma Bragado:** Writing – review & editing, Writing – original draft, Visualization, Validation, Supervision, Project administration, Methodology, Investigation, Formal analysis, Data curation, Conceptualization. **Alvaro Gutierrez-Uzquiza:** Writing – review & editing, Writing – original draft, Visualization, Validation, Supervision, Software, Resources, Project administration, Methodology, Investigation, Funding acquisition, Formal analysis, Data curation, Conceptualization.

Declaration of competing interest

The authors declare that they have no known competing financial interests or personal relationships that could have appeared to influence the work reported in this paper.

Acknowledgments

We would like to acknowledge the computing resources and technical support provided by the SCBI (Supercomputing and Bioinformatics) center of the University of Málaga in the Red Española de Supercomputación (RES). We thank the Genetic and Genomic Facility at UCM (Madrid, Spain) for the CRISPR/Cas9 screenings NSG sequencing and the Bioinformatics for Genomics and Proteomics Unit at CNB–CSIC facility (Madrid, Spain) for the analysis of CRISPR/Cas9 raw data.

Appendix A. Supplementary data

Supplementary data to this article can be found online at https://doi.org/10.1016/j.canlet.2024.216776.

References

[1] H. Sung, J. Ferlay, R.L. Siegel, M. Laversanne, I. Soerjomataram, A. Jemal, F. Bray, Global cancer statistics 2020: GLOBOCAN estimates of incidence and mortality worldwide for 36 cancers in 185 countries, CA A Cancer J. Clin. 71 (2021) 209–249, https://doi.org/10.3322/caac.21660.

[2] J.S. de Bono, C.J. Logothetis, A. Molina, K. Fizazi, S. North, L. Chu, K.N. Chi, R. J. Jones, O.B. Goodman, F. Saad, J.N. Staffurth, P. Mainwaring, S. Harland, T. W. Flaig, T.E. Hutson, T. Cheng, H. Patterson, J.D. Hainsworth, C.J. Ryan, C. N. Sternberg, S.L. Ellard, A. Fléchon, M. Saleh, M. Scholz, E. Efstathiou, A. Zivi, D. Bianchini, Y. Loriot, N. Chieffo, T. Kheoh, C.M. Haqq, H.I. Scher, COU-AA-301 Investigators, Abiraterone and increased survival in metastatic prostate cancer, N. Engl. J. Med. 364 (2011) 1995–2005, https://doi.org/10.1056/NEJMoa1014618.

[3] N.D. James, M.R. Sydes, N.W. Clarke, M.D. Mason, D.P. Dearnaley, M.R. Spears, A. W.S. Ritchie, C.C. Parker, J.M. Russell, G. Attard, J. de Bono, W. Cross, R.J. Jones, G. Thalmann, C. Amos, D. Matheson, R. Millman, M. Alzouebi, S. Beesley, A. J. Birtle, S. Brock, R. Cathomas, P. Chakraborti, S. Chowdhury, A. Cook, T. Elliott, J. Gale, S. Gibbs, J.D. Graham, J. Hetherington, R. Hughes, R. Laing, F. McKinna, D.B. McLaren, J.M. O'Sullivan, O. Parikh, C. Peedell, A. Protheroe, A.J. Robinson, N. Srihari, R. Srinivasan, J. Staffurth, S. Sundar, S. Tolan, D. Tsang, J. Wagstaff, M.

K.B. Parmar, Addition of docetaxel, zoledronic acid, or both to first-line long-term hormone therapy in prostate cancer (STAMPEDE): survival results from an adaptive, multiarm, multistage, platform randomised controlled trial, Lancet 387 (2016) 1163–1177, https://doi.org/10.1016/S0140-6736(15)01037-5.
[4] T.M. Beer, A.J. Armstrong, D.E. Rathkopf, Y. Loriot, C.N. Sternberg, C.S. Higano, P. Iversen, S. Bhattacharya, J. Carles, S. Chowdhury, I.D. Davis, J.S. de Bono, C. P. Evans, K. Fizazi, A.M. Joshua, C.-S. Kim, G. Kimura, P. Mainwaring, H. Mansbach, K. Miller, S.B. Noonberg, F. Perabo, D. Phung, F. Saad, H.I. Scher, M.-E. Taplin, P.M. Venner, B. Tombal, PREVAIL Investigators, Enzalutamide in metastatic prostate cancer before chemotherapy, N. Engl. J. Med. 371 (2014) 424–433, https://doi.org/10.1056/NEJMoa1405095.
[5] J. Massagué, A.C. Obenauf, Metastatic colonization by circulating tumour cells, Nature 529 (2016) 298–306, https://doi.org/10.1038/nature17038.
[6] O. Sartor, J.S. de Bono, Metastatic prostate cancer, N. Engl. J. Med. 378 (2018) 645–657, https://doi.org/10.1056/NEJMra1701695.
[7] S.Y. Ku, S. Rosario, Y. Wang, P. Mu, M. Seshadri, Z.W. Goodrich, M.M. Goodrich, D. P. Labbé, E.C. Gomez, J. Wang, H.W. Long, B. Xu, M. Brown, M. Loda, C. L. Sawyers, L. Ellis, D.W. Goodrich, Rb1 and Trp53 cooperate to suppress prostate cancer lineage plasticity, metastasis, and antiandrogen resistance, Science 355 (2017) 78–83, https://doi.org/10.1126/science.aah4199.
[8] D. Robinson, E.M. Van Allen, Y.-M. Wu, N. Schultz, R.J. Lonigro, J.-M. Mosquera, B. Montgomery, M.-E. Taplin, C.C. Pritchard, G. Attard, H. Beltran, W. Abida, R. K. Bradley, J. Vinson, X. Cao, P. Vats, L.P. Kunju, M. Hussain, F.Y. Feng, S. A. Tomlins, K.A. Cooney, D.C. Smith, C. Brennan, J. Siddiqui, R. Mehra, Y. Chen, D. E. Rathkopf, M.J. Morris, S.B. Solomon, J.C. Durack, V.E. Reuter, A. Gopalan, J. Gao, M. Loda, R.T. Lis, M. Bowden, S.P. Balk, G. Gaviola, C. Sougnez, M. Gupta, E.Y. Yu, E.A. Mostaghel, H.H. Cheng, H. Mulcahy, L.D. True, S.R. Plymate, H. Dvinge, R. Ferraldeschi, P. Flohr, S. Miranda, Z. Zafeiriou, N. Tunariu, J. Mateo, R. Perez-Lopez, F. Demichelis, B.D. Robinson, M. Schiffman, D.M. Nanus, S. T. Tagawa, A. Sigaras, K.W. Eng, O. Elemento, A. Sboner, E.I. Heath, H.I. Scher, K. J. Pienta, P. Kantoff, J.S. de Bono, M.A. Rubin, P.S. Nelson, L.A. Garraway, C. L. Sawyers, A.M. Chinnaiyan, Integrative clinical genomics of advanced prostate cancer, Cell 161 (2015) 1215–1228, https://doi.org/10.1016/j.cell.2015.05.001.
[9] S. Varambally, S.M. Dhanasekaran, M. Zhou, T.R. Barrette, C. Kumar-Sinha, M. G. Sanda, D. Ghosh, K.J. Pienta, R.G.A.B. Sewalt, A.P. Otte, M.A. Rubin, A. M. Chinnaiyan, The polycomb group protein EZH2 is involved in progression of prostate cancer, Nature 419 (2002) 624–629, https://doi.org/10.1038/nature01075.
[10] D. Ren, Y. Dai, Q. Yang, X. Zhang, W. Guo, L. Ye, S. Huang, X. Chen, Y. Lai, H. Du, C. Lin, X. Peng, L. Song, Wnt5a induces and maintains prostate cancer cells dormancy in bone, J. Exp. Med. 216 (2019) 428–449, https://doi.org/10.1084/jem.20180661.
[11] S. Garcia-Garcia, M. Rodrigo-Faus, N. Fonseca, S. Manzano, B. Győrffy, A. Ocaña, P. Bragado, A. Porras, A. Gutierrez-Uzquiza, HGK promotes metastatic dissemination in prostate cancer, Sci. Rep. 11 (2021) 12287, https://doi.org/10.1038/s41598-021-91292-2.
[12] M. Chen, L. Wan, J. Zhang, J. Zhang, L. Mendez, J.G. Clohessy, K. Berry, J. Victor, Q. Yin, Y. Zhu, W. Wei, P.P. Pandolfi, Deregulated PP1α phosphatase activity towards MAPK activation is antagonized by a tumor suppressive failsafe mechanism, Nat. Commun. 9 (2018) 159, https://doi.org/10.1038/s41467-017-02272-y.
[13] M. Jinek, K. Chylinski, I. Fonfara, M. Hauer, J.A. Doudna, E. Charpentier, A programmable dual-RNA-guided DNA endonuclease in adaptive bacterial immunity, Science 337 (2012) 816–821, https://doi.org/10.1126/science.1225829.
[14] N.E. Sanjana, O. Shalem, F. Zhang, Improved vectors and genome-wide libraries for CRISPR screening, Nat. Methods 11 (2014) 783–784, https://doi.org/10.1038/nmeth.3047.
[15] K. Tzelepis, H. Koike-Yusa, E. De Braekeleer, Y. Li, E. Metzakopian, O.M. Dovey, A. Mupo, V. Grinkevich, M. Li, M. Mazan, M. Gozdecka, S. Ohnishi, J. Cooper, M. Patel, T. McKerrell, B. Chen, A.F. Domingues, P. Gallipoli, S. Teichmann, H. Ponstingl, U. McDermott, J. Saez-Rodriguez, B.J.P. Huntly, F. Iorio, C. Pina, G. S. Vassiliou, K. Yusa, A CRISPR dropout screen identifies genetic vulnerabilities and therapeutic targets in acute myeloid leukemia, Cell Rep. 17 (2016) 1193–1205, https://doi.org/10.1016/j.celrep.2016.09.079.
[16] C. Cheng, X. Pei, S.-W. Li, J. Yang, C. Li, J. Tang, K. Hu, G. Huang, W.-P. Min, Y. Sang, CRISPR/Cas9 library screening uncovered methylated PKP2 as a critical driver of lung cancer radioresistance by stabilizing β-catenin, Oncogene 40 (2021) 2842–2857, https://doi.org/10.1038/s41388-021-01692-x.
[17] W. Li, H. Xu, T. Xiao, L. Cong, M.I. Love, F. Zhang, R.A. Irizarry, J.S. Liu, M. Brown, X.S. Liu, MAGeCK enables robust identification of essential genes from genome-scale CRISPR/Cas9 knockout screens, Genome Biol. 15 (2014) 554, https://doi.org/10.1186/s13059-014-0554-4.
[18] N. Palao, C. Sequera, Á.M. Cuesta, C. Baquero, P. Bragado, A. Gutierrez-Uzquiza, A. Sánchez, C. Guerrero, A. Porras, C3G down-regulation enhances pro-migratory and stemness properties of oval cells by promoting an epithelial-mesenchymal-like process, Int. J. Biol. Sci. 18 (2022) 5873–5884, https://doi.org/10.7150/ijbs.73192.
[19] P. Bragado, Y. Estrada, F. Parikh, S. Krause, C. Capobianco, H.G. Farina, D. M. Schewe, J.A. Aguirre-Ghiso, TGF-β2 dictates disseminated tumour cell fate in target organs through TGF-β-RIII and p38α/β signalling, Nat. Cell Biol. 15 (2013) 1351–1361, https://doi.org/10.1038/ncb2861.
[20] J.A. Nemeth, J.F. Harb, U. Barroso, Z. He, D.J. Grignon, M.L. Cher, Severe combined immunodeficient-hu model of human prostate cancer metastasis to human bone, Cancer Res. 59 (1999) 1987–1993.
[21] A. Dobin, C.A. Davis, F. Schlesinger, J. Drenkow, C. Zaleski, S. Jha, P. Batut, M. Chaisson, T.R. Gingeras, STAR: ultrafast universal RNA-seq aligner, Bioinformatics 29 (2013) 15–21, https://doi.org/10.1093/bioinformatics/bts635.
[22] M.I. Love, W. Huber, S. Anders, Moderated estimation of fold change and dispersion for RNA-seq data with DESeq2, Genome Biol. 15 (2014) 550, https://doi.org/10.1186/s13059-014-0550-8.
[23] R Core Team, R: A Language and Environment for Statistical Computing, R Foundation for Statistical Computing, Vienna, AustriaURL, 2021. https://www.R-project.org/.
[24] T. Wu, E. Hu, S. Xu, M. Chen, P. Guo, Z. Dai, T. Feng, L. Zhou, W. Tang, L. Zhan, X. Fu, S. Liu, X. Bo, G. Yu, clusterProfiler 4.0: a universal enrichment tool for interpreting omics data, Innovation 2 (2021) 100141, https://doi.org/10.1016/j.xinn.2021.100141.
[25] M. Carlson, org.Hs.eg.db: Genome Wide Annotation for Human, 2019. R package version 3.8.2., (n.d.).
[26] S. Sayols, Rrvgo: a Bioconductor Package to Reduce and Visualize Gene Ontology Terms, 2020. https://ssayols.github.io/rrvgo.
[27] F. Hammal, P. de Langen, A. Bergon, F. Lopez, B. Ballester, ReMap 2022: a database of Human, Mouse, Drosophila and Arabidopsis regulatory regions from an integrative analysis of DNA-binding sequencing experiments, Nucleic Acids Res. 50 (2021) D316–D325, https://doi.org/10.1093/nar/gkab996.
[28] M. Lawrence, W. Huber, H. Pagès, P. Aboyoun, M. Carlson, R. Gentleman, M. T. Morgan, V.J. Carey, Software for computing and annotating genomic ranges, PLoS Comput. Biol. 9 (2013) e1003118, https://doi.org/10.1371/journal.pcbi.1003118.
[29] P. Badia-i-Mompel, J. Vélez Santiago, J. Braunger, C. Geiss, D. Dimitrov, S. Müller-Dott, P. Taus, A. Dugourd, C.H. Holland, R.O. Ramirez Flores, J. Saez-Rodriguez, decoupleR: ensemble of computational methods to infer biological activities from omics data, Bioinformatics Adv. 2 (2022), https://doi.org/10.1093/bioadv/vbac016 vbac016.
[30] W.-J. Li, Y.-H. He, J.-J. Yang, G.-S. Hu, Y.-A. Lin, T. Ran, B.-L. Peng, B.-L. Xie, M.-F. Huang, X. Gao, H.-H. Huang, H.H. Zhu, F. Ye, W. Liu, Profiling PRMT methylome reveals roles of hnRNPA1 arginine methylation in RNA splicing and cell growth, Nat. Commun. 12 (2021), https://doi.org/10.1038/s41467-021-21963-1, 1946.
[31] P. Shannon, A. Markiel, O. Ozier, N.S. Baliga, J.T. Wang, D. Ramage, N. Amin, B. Schwikowski, T. Ideker, Cytoscape: a software environment for integrated models of biomolecular interaction networks, Genome Res. 13 (2003) 2498–2504, https://doi.org/10.1101/gr.1239303.
[32] Y. Zhou, B. Zhou, L. Pache, M. Chang, A.H. Khodabakhshi, O. Tanaseichuk, C. Benner, S.K. Chanda, Metascape provides a biologist-oriented resource for the analysis of systems-level datasets, Nat. Commun. 10 (2019) 1523, https://doi.org/10.1038/s41467-019-09234-6.
[33] A. Subramanian, P. Tamayo, V.K. Mootha, S. Mukherjee, B.L. Ebert, M.A. Gillette, A. Paulovich, S.L. Pomeroy, T.R. Golub, E.S. Lander, J.P. Mesirov, Gene set enrichment analysis: a knowledge-based approach for interpreting genome-wide expression profiles, Proc. Natl. Acad. Sci. U.S.A. 102 (2005) 15545–15550, https://doi.org/10.1073/pnas.0506580102.
[34] Venny, Venn diagrams for comparing lists. By juan Carlos oliveros. https://bioinfogp.cnb.csic.es/tools/venny_old/venny.php, March 31, 2023.
[35] D.S. Chandrashekar, B. Bashel, S.A.H. Balasubramanya, C.J. Creighton, I. Ponce-Rodriguez, B.V.S.K. Chakravarthi, S. Varambally, UALCAN: a portal for facilitating tumor subgroup gene expression and survival analyses, Neoplasia 19 (2017) 649–658, https://doi.org/10.1016/j.neo.2017.05.002.
[36] D.S. Chandrashekar, S.K. Karthikeyan, P.K. Korla, H. Patel, A.R. Shovon, M. Athar, G.J. Netto, Z.S. Qin, S. Kumar, U. Manne, C.J. Creighton, S. Varambally, UALCAN: an update to the integrated cancer data analysis platform, Neoplasia 25 (2022) 18–27, https://doi.org/10.1016/j.neo.2022.01.001.
[37] K.-H. Tsui, P.-L. Chang, T.-H. Feng, L.-C. Chung, H.-C. Sung, H.-H. Juang, Evaluating the function of matriptase and N-acetylglucosaminyltransferase V in prostate cancer metastasis, Anticancer Res. 28 (2008) 1993–1999.
[38] M.E. Kaighn, K.S. Narayan, Y. Ohnuki, J.F. Lechner, L.W. Jones, Establishment and characterization of a human prostatic carcinoma cell line (PC-3), Invest. Urol. 17 (1979) 16–23.
[39] K.R. Stone, D.D. Mickey, H. Wunderli, G.H. Mickey, D.F. Paulson, Isolation of a human prostate carcinoma cell line (DU 145), Int. J. Cancer 21 (1978) 274–281, https://doi.org/10.1002/ijc.2910210305.
[40] K. Jain, S.G. Clarke, PRMT7 as a unique member of the protein arginine methyltransferase family: a review, Arch. Biochem. Biophys. 665 (2019) 36–45, https://doi.org/10.1016/j.abb.2019.02.014.
[41] R. Yao, H. Jiang, Y. Ma, L. Wang, L. Wang, J. Du, P. Hou, Y. Gao, L. Zhao, G. Wang, Y. Zhang, D.-X. Liu, B. Huang, J. Lu, PRMT7 induces epithelial-to-mesenchymal transition and promotes metastasis in breast cancer, Cancer Res. 74 (2014) 5656–5667, https://doi.org/10.1158/0008-5472.CAN-14-0800.
[42] D. Cheng, Z. He, L. Zheng, D. Xie, S. Dong, P. Zhang, PRMT7 contributes to the metastasis phenotype in human non-small-cell lung cancer cells possibly through the interaction with HSPA5 and EEF2, OncoTargets Ther. 11 (2018) 4869–4876, https://doi.org/10.2147/OTT.S166412.
[43] K. Jain, S.G. Clarke, PRMT7 as a unique member of the protein arginine methyltransferase family: a review, Arch. Biochem. Biophys. 665 (2019) 36–45, https://doi.org/10.1016/j.abb.2019.02.014.
[44] F. Liu, L. Wan, H. Zou, Z. Pan, W. Zhou, X. Lu, PRMT7 promotes the growth of renal cell carcinoma through modulating the β-catenin/C-MYC axis, Int. J. Biochem. Cell Biol. 120 (2020) 105686, https://doi.org/10.1016/j.biocel.2020.105686.
[46] A. Gutierrez-Uzquiza, C. Lopez-Haber, D.L. Jernigan, A. Fatatis, M.G. Kazanietz, PKCε is an essential mediator of prostate cancer bone metastasis, Mol. Cancer Res. 13 (2015) 1336–1346, https://doi.org/10.1158/1541-7786.MCR-15-0111.

[47] H. Hamidi, J. Ivaska, Every step of the way: integrins in cancer progression and metastasis, Nat. Rev. Cancer 18 (2018) 533–548, https://doi.org/10.1038/s41568-018-0038-z.
[48] R.O. Hynes, Integrins: bidirectional, allosteric signaling machines, Cell 110 (2002) 673–687, https://doi.org/10.1016/S0092-8674(02)00971-6.
[49] S.-H. Lee, T.-Y. Chen, S.S. Dhar, B. Gu, K. Chen, Y.Z. Kim, W. Li, M.G. Lee, A feedback loop comprising PRMT7 and miR-24-2 interplays with Oct4, Nanog, Klf4 and c-Myc to regulate stemness, Nucleic Acids Res. 44 (2016) 10603–10618, https://doi.org/10.1093/nar/gkw788.
[50] A.B. El-Khoueiry, J. Clarke, T. Neff, T. Crossman, N. Ratia, C. Rathi, P. Noto, A. Tarkar, I. Garrido-Laguna, E. Calvo, J. Rodón, B. Tran, P.J. O'Dwyer, A. Cuker, A.R. Abdul Razak, Phase 1 study of GSK3368715, a type I PRMT inhibitor, in patients with advanced solid tumors, Br. J. Cancer 129 (2023) 309–317, https://doi.org/10.1038/s41416-023-02276-0.
[51] G.P. Gupta, J. Massagué, Cancer metastasis: building a framework, Cell 127 (2006) 679–695, https://doi.org/10.1016/j.cell.2006.11.001.
[52] R.M. Baldwin, N. Haghandish, M. Daneshmand, S. Amin, G. Paris, T.J. Falls, J. C. Bell, S. Islam, J. Côté, Protein arginine methyltransferase 7 promotes breast cancer cell invasion through the induction of MMP9 expression, Oncotarget 6 (2014) 3013–3032, https://doi.org/10.18632/oncotarget.3072.
[53] R.K. Bikkavilli, S. Avasarala, M. Vanscoyk, M. Sechler, N. Kelley, C.C. Malbon, R. A. Winn, Dishevelled3 is a novel arginine methyl transferase substrate, Sci. Rep. 2 (2012) 805, https://doi.org/10.1038/srep00805.
[54] Y.-E. Leem, J.-H. Bae, H.-J. Jeong, J.-S. Kang, PRMT7 deficiency enhances adipogenesis through modulation of C/EBP-β, Biochem. Biophys. Res. Commun. 517 (2019) 484–490, https://doi.org/10.1016/j.bbrc.2019.07.096.
[55] A. Gharibi, S. La Kim, J. Molnar, D. Brambilla, Y. Adamian, M. Hoover, J. Hong, J. Lin, L. Wolfenden, J.A. Kelber, ITGA1 is a pre-malignant biomarker that promotes therapy resistance and metastatic potential in pancreatic cancer, Sci. Rep. 7 (2017) 10060, https://doi.org/10.1038/s41598-017-09946-z.
[56] Y.W. Moon, G. Rao, J.J. Kim, H.-S. Shim, K.-S. Park, S.S. An, B. Kim, P.S. Steeg, S. Sarfaraz, L. Changwoo Lee, D. Voeller, E.Y. Choi, J. Luo, D. Palmieri, H. C. Chung, J.-H. Kim, Y. Wang, G. Giaccone, LAMC2 enhances the metastatic potential of lung adenocarcinoma, Cell Death Differ. 22 (2015) 1341–1352, https://doi.org/10.1038/cdd.2014.228.
[57] R.J. Rebello, C. Oing, K.E. Knudsen, S. Loeb, D.C. Johnson, R.E. Reiter, S. Gillessen, T. Van der Kwast, R.G. Bristow, Prostate cancer, Nat. Rev. Dis. Prim. 7 (2021) 9, https://doi.org/10.1038/s41572-020-00243-0.
[58] G. Klein, C.A. Müller, E. Tillet, M.-L. Chu, R. Timpl, Collagen type VI in the human bone marrow microenvironment: a strong cytoadhesive component, Blood 86 (1995) 1740–1748, https://doi.org/10.1182/blood.V86.5.1740.bloodjournal8651740.
[59] F. Chen, W. Xiong, K. Dou, Q. Ran, Knockdown of FOXK1 suppresses proliferation, migration, and invasion in prostate cancer cells, Oncol. Res. 25 (2017) 1261–1267, https://doi.org/10.3727/096504017X14871164924588.
[60] Y. Gu, J. Jiang, C. Liang, TFAP4 promotes the growth of prostate cancer cells by upregulating FOXK1, Exp. Ther. Med. 22 (2021) 1299, https://doi.org/10.3892/etm.2021.10734.
[61] X. Li, N. Mo, Z. Li, Ginsenosides: potential therapeutic source for fibrosis-associated human diseases, J Ginseng. Res. 44 (2020) 386–398, https://doi.org/10.1016/j.jgr.2019.12.003.
[62] A.E. Raposo, S.C. Piller, Protein arginine methylation: an emerging regulator of the cell cycle, Cell Div. 13 (2018) 3, https://doi.org/10.1186/s13008-018-0036-2.
[63] Elucidating the role of PRMTs in prostate cancer using open access databases and a patient cohort dataset, Histol. Histopathol. 38 (2022) 287–302, https://doi.org/10.14670/HH-18-513.